



HOST UNIVERSITY: Ghent University

FACULTY: Faculty of Engineering and Architecture

DEPARTMENT: Department of Flow, Heat and Combustion Mechanics

Academic Year 2018-2020

Analysis of Travelling Fires using CFD Simulations and Comparison to the Travelling Fire Methodology

RAMSAMY Vinayagum Reyalen

Promoters: Prof Dr. Ir. Bart Merci and Prof. Dr. Ir.-arch Emmanuel Annerel

Master thesis submitted in the Erasmus+ Study Programme

International Master of Science in Fire Safety Engineering

DISCLAIMER

This thesis is submitted in partial fulfilment of the requirements for the degree of *The International Master of Science in Fire Safety Engineering (IMFSE)*. This thesis has never been submitted for any degree or examination to any other University/programme. The author declares that this thesis is original work except where stated. This declaration constitutes an assertion that full and accurate references and citations have been included for all material, directly included and indirectly contributing to the thesis. The author gives permission to make this master thesis available for consultation and to copy parts of this master thesis for personal use. In the case of any other use, the limitations of the copyright have to be respected, in particular with regard to the obligation to state expressly the source when quoting results from this master thesis. The thesis supervisor must be informed when data or results are used.

Read and approved,

A handwritten signature in blue ink, appearing to read 'Ramsamy', with a horizontal line underneath the name.

RAMSAMY Vinayagum Reyalen
20/04/2020

1 ABSTRACT

As open-plan compartments become increasingly common in the built environment, it is important to question whether the assumptions embedded in fire standards remain valid. In contrast to a typical room, where a homogenous temperature distribution may be expected post-flashover, travelling fires are characterised by a flame front that progressively spreads across the room, leading to regions of high and low temperatures, at different points in time and space.

This study uses the Fire Dynamics Simulator (FDS) to investigate travelling fires, highlighting the main parameters influencing the temperature profile within the enclosure. Several simulations with different geometries, Heat Release Rate per Unit Area (HRRPUA), and ventilation configurations are explored. It is observed that the fire behaviour and the temperature profile are highly sensitive to the ventilation conditions. The location and size of the openings have a large impact on the flow field causing peak temperatures ranging from 600 to 1300°C to develop. A transition from travelling fire behaviour to localised flashover is identified in compartments with closed recesses. Significant non-axisymmetric ceiling jets are recorded in some simulations causing increased thermal exposure to certain sections of the ceiling.

Next, the Travelling Fire Methodology (TFM) is implemented and the results are compared with the numerical simulation output. A time-offset linked to the fixed fire spread rate assumption of the TFM is observed upon comparison of the results. The flame spread rates derived from the simulation data reveal a non-constant value during the fire event. It is also noted that the far-field temperatures are consistently underpredicted by the TFM.

The research concludes that accurate representation of the fire spread rate is critical in achieving reasonable results from the methodology. The inability to incorporate the effects of ventilation on the temperature profile is identified as being a major shortcoming of the TFM.

Keywords: *Travelling fires, Fire Dynamics Simulator (FDS), Travelling Fire Methodology (TFM), Large compartments, fire spread rate*

Word Count: 16204 words

IMFSE Master Thesis Declaration

This form has been developed in the context of the unforeseen circumstances due to Covid-19, necessitating a reduction of practical project work (whether it be laboratory based, computational, or fieldwork) during the master thesis semester. It acts as a record of the impact on the master thesis. The form has been completed by the student and verified by the supervisor. **A copy of the signed form is included behind the abstract in the dissertation.**

Name: **RAMSAMY Vinayagum Reyalen**

Work completed

All items of wholly, or partially completed work must be listed, indicating the percentage completion for each task. **Please take care to provide a full detailed list of all work done.**

To map available theoretical models of travelling fires through a literature study, summarising their theoretical backgrounds and highlighting the application limits.	100%
To study a range of travelling fires using Computational Fluid Dynamics (CFD) by altering the geometry and fire characteristics.	100%
To compare the results of the CFD study with the prediction of the Travelling Fire Methodology (TFM).	100%
To identify and investigate key parameters for accurate prediction of the theoretical models.	100%

Work not commenced

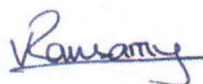
Any items of outstanding work that have not been started should be listed here.

N/A

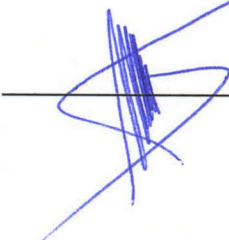
Declaration

To the best of our knowledge, this form is an accurate record of the project status on 20/04/2020

Student:



Supervisor:



2 TABLE OF CONTENTS

1	Abstract.....	1
3	Introduction	5
3.1	Aims and Objectives.....	5
4	Literature Review.....	6
4.1	What are Travelling fires?.....	6
4.2	Theoretical models	6
4.2.1	Migrating Firecell Model (MFM).....	6
4.2.2	Travelling Fires Methodology (TFM).....	6
4.2.3	Extended Travelling Fires Methodology (ETFM).....	7
4.2.4	Improved Travelling Fire Methodology (iTFM).....	8
4.3	Travelling Fires – Parameters of interest.....	8
4.3.1	Ventilation Openings.....	8
4.3.2	Geometry of Compartment	9
4.3.3	Heat Release Rate (HRR).....	10
4.4	Methods of Research.....	11
4.4.1	Full -Scale Tests	11
4.4.2	Reduced Scaled- Experiments.....	11
4.4.3	Numerical Study.....	11
4.5	Current Limitations of Travelling Fire Research.....	12
	• Validation of Results	12
	• Availability of Experimental Results – Lack of spatial resolution.....	12
	• Parameter Sensitivity.....	12
	• Simplification of Fuel Packages.....	12
5	Methodology.....	13
5.1	FDS Model Development	13
5.1.1	Fire Dynamics Simulator (FDS) and High-Performance Computing (HPC) Infrastructure 13	
5.1.2	Geometry and Boundary Conditions	13
5.1.3	Fire Characteristics.....	14
5.1.4	Fire Spread Modelling.....	15
5.1.5	Mesh Treatment	16
5.1.6	Simulation Input Parameters	21
5.2	Application of the Travelling Fire Methodology	24
5.2.1	Travelling Fire Methodology (TFM).....	24

6	Results And Discussion.....	27
6.1	Analysis of Travelling Fire Behaviour	27
6.1.1	Control Case - Temperature Profile	27
6.1.2	Ventilation Opening Configurations	29
6.1.3	Compartment ceiling height and travelling fire behaviour.....	35
6.1.4	HRRPUA and Travelling Fire Behaviour.....	37
6.2	Implementation of Travelling Fire Methodology.....	41
6.2.1	Ventilation Configurations and TFM.....	42
6.2.2	Compartment Height and TFM	43
6.2.3	Increased HRRPUA and TFM	44
6.2.4	Compartment Geometry and TFM.....	45
6.3	TFM + Hasemi Model for Flame Extension	46
6.4	Fire spread rates	47
7	Conclusion And Future works	52
8	Acknowledgements.....	54
9	References	55
10	APPENDICES	58
10.1	Compartment Dimensions	58
10.2	Fire Spread Rate in TFM Methodology	59
10.3	Computational Domain Optimisation	60
10.4	Compartment Geometry for Mesh Sensitivity Study.....	61
10.5	FDS Code (Extract of Control Case Provided).....	61
10.6	HPC Infrastructure Script (Sample)	65

3 INTRODUCTION

The focus of fire research has, traditionally, been targeted towards understanding the intricacies and dynamics associated to fire development in enclosures commonly encountered in the built environment. Logically, the brunt of experimental tests conducted were aimed at replicating small compartments with boxlike geometries [1], for which the assumption of a spatially homogenous burning and temperature within the enclosure was deemed conservative for structural fire analysis. The uniform burning and homogenous temperature distribution have, as a result, become embedded in fire design standards [2] and subsequently justified the adoption of monotonically increasing temperature time curves, such as the standard time-temperature curve, external fire curve and the hydrocarbon curve.

However, the validity of such assumptions breaks down in large compartments, where real fires do not burn simultaneously throughout the compartment, but rather travel across the room, thus leading to regions of higher and lower temperatures [3] both spatially and temporally. Such fire behaviours, labelled 'travelling fires', have been observed both experimentally in Cardington [4] and Dalmarnock fire tests [5] as well as in large accidental fires, such as the Ghost Ship Warehouse Fire in the U.S.A in 2016 [6], TU Delft in the Netherlands in 2008 [7], the Windsor Tower in Spain in 2005 [8] and the World Trade Center in New York in 2001 [9].

While the inclusion of the parametric temperature-time curves in the Eurocode 1 [10] has partially addressed the transient nature of the temperature within an enclosure, its narrow applicability limits preclude its use as a blanket solution, often excluding compartments where travelling fire behaviour would be expected. This issue stems from the fact that current understanding of compartment fire behaviour comes mainly from experiments involving near cubical compartments [11]. It is therefore critical that the evolution of traveling fires, associated with large compartments, be investigated and explored, in order to better define the prevailing temperature field and characterise more accurately the actual building performance of a structure under fire conditions [2]. With both an increased propensity to build large, open plan structures and surveys [12] showing that modern structures fall increasingly outside the applicability limits of the Eurocode, the need to capture the particularities of travelling fires is only a natural evolution towards adaptation to a shifting architectural environment.

Owing to the high cost associated to full scale testing for this study, this thesis attempts to gather and interpret data using numerical means in order to identify the impact of physical factors on the behaviour of travelling fires and provide a preliminary validation of the Travelling Fire Methodology (TFM). The thesis focuses on the effect of ventilation, geometry and heat release rate per unit area on travelling fire behaviour as well as fire spread rates on the TFM results.

3.1 AIMS AND OBJECTIVES

The overall aim of the thesis is to develop a deeper understanding of travelling fires through numerical analysis. A four-tiered approach is used to that effect:

1. To map available theoretical models of travelling fires through a literature study, summarising their theoretical backgrounds and highlighting the application limits.
2. To study a range of travelling fires using Computational Fluid Dynamics (CFD) by altering the geometry and fire characteristics.
3. To compare the results of the CFD study with the prediction of the Travelling Fire Methodology (TFM).
4. To identify and investigate key parameters for accurate prediction of the theoretical models.

4 LITERATURE REVIEW

4.1 WHAT ARE TRAVELLING FIRES?

Stern-Gottfried describes travelling fires as those that do not burn simultaneously throughout a compartment but instead, move across floor plates as the flame spreads, burning over a limited area at any one time [5]. Such fires are contrasted with the flashover fire event that usually involves the whole compartment at once.

4.2 THEORETICAL MODELS

4.2.1 Migrating Firecell Model (MFM)

One of the first documents linking structural design to travelling fires was put forward by Clifton [13] in a report called “Fire Models for Large Firecells” as part of a research programme at HERA in New Zealand. The objective of the study was to understand the behaviour of steel elements under fire conditions; the report provided a method which employed two different fire models and several rules to represent the temperature-time relationship of a travelling fire. The approach consisted of subdividing the total floor area of a compartment, defined as a firecell by Clifton, into a given number of design areas. The design areas would then be assigned one of the following attributes namely: fire, burned out, preheat or smoke logged. Based on these attributes, the temperature-time curves were derived using the newly proposed fire models.

One of the main shortcomings of the model, as acknowledged by Clifton, was the lack of experimental data available; several assumptions pertaining to fire size, fire spread and ventilation conditions were required in order to build the model. While analyses conducted by Moss *et al.* using the migrating firecell method have produced somewhat realistic results when validated against some Cardington tests [14], the study concluded that “they could not be related to any directly comparable experimental results”. For this reason, it is important to verify the validity of the model when challenged with a broad range of varying parameters. The list below provides a list of inherent assumptions used in the MFM [15] that warrant further validation while providing new avenues to explore in travelling fire modelling.

1. Preheat and delayed cooling periods are assigned within temperature band of 400 to 800°C
2. Window breakage when gas temperatures at the windows reached 350°C
3. Individual design area size is fixed at 50m².

4.2.2 Travelling Fires Methodology (TFM)

In 2010, during the SFPE Conference held in Lund, Sweden, a renewed approach that encompassed both uniform burning and travelling fires was proposed by Stern-Gottfried *et al.* [16]; the paper established a framework to calculate the thermal environment and corresponding structural response for a wide range of fires in enclosures. It established that uniform temperature assumption does not necessarily lead to more conservative structural performance results. One of the main distinct traits of the TFM was the classification of the temperature field with respect to its influence on the structure, rather than being characterised by the state of the fire as performed in the MFM approach. This allowed the methodology to circumvent the inaccuracies associated with flame temperature prediction of most fire models [16]. Using the TFM, the temperature field was divided into a near field, where a structural element is directly exposed to the flames, and the far field, where the element is exposed to hot gases (typically smoke layer).

The travelling nature of the fire was characterised and determined by defining a percentage representative of the fraction of total floor compartment burning at any time. This implied that a constant burning area is assumed over the entire fire duration. Further assumptions include:

1. A uniform fuel load across the fire path.
2. A burning time based on fuel load density and Heat Release Rate (HRR) only.
3. Very fast growth and decay phase.
4. Burning time independent of burning area.

The calculation of the far field temperature is calculated in the model by employing the ceiling jet correlation developed by Alpert while the near field is assumed to be equal to the flame temperature. Although the Alpert correlations provide a relatively simple estimation of the gas temperatures based on only three variables (see Eq. 1), its use also entails that several other factors that could potentially affect the temperature field are ignored.

$$T_{gas} - T_{\infty} = 5.38 \frac{\dot{Q}_3^{\frac{2}{3}} H^{\frac{5}{3}}}{\left(\frac{r}{H}\right)^{2/3}}, \quad r/H > 0.18 \quad \text{Eq. 1 [17]}$$

These intrinsic assumptions should be assessed in the context of their use for travelling fires. Alpert [18] noted that the correlation was appropriate subject to restrictions, some of which are listed below:

1. Ceilings are smooth.
2. Fire intensity does not double in less than one minute.
3. Wall to wall distance is 2 to 4 ceiling heights.

Most importantly, his paper highlighted that drafts induced by room ventilation were not included when formulating the equations. It is, however, known that ventilation does affect the temperature evolution; this has been confirmed by Welch *et al.* [19] in large scale fire tests. Studies conducted by Johansson *et al.* [20] have shown that the correlations presented by Alpert underestimated the maximum temperature by 30 to 50% when compared to results from numerical experiments. It would therefore be interesting to investigate the predictive capabilities of this methodology.

It should be noted that, for structural analysis, the far field temperature, T_{ff} , according to the TFM methodology, is condensed into a single value by using a fourth power average of T_{max} in an attempt to bias high temperatures and simplify further processing of the information, as shown Eq. 2.

$$T_{ff} = \frac{\left[\int_{n_f}^{ff} (T_{max})^4 dr \right]^{\frac{1}{4}}}{(r_{ff} - r_{n_f})^{\frac{1}{4}}} \quad \text{Eq. 2 [16]}$$

4.2.3 Extended Travelling Fires Methodology (ETFM)

The ETFM, much like the TFM distinguishes between the near field region and far field region. In this methodology, the near field region values are derived using a variant of Hasemi's localised fire model whereas the far field is based on a zone model approach [21]. The ETFM framework allows for variable temperatures in the near field, unlike that of the TFM, which assumed a constant value between 800-1200°C. Most importantly, due to the introduction of a zone model to compute the far field values, the effects of smoke accumulation under the ceiling could also be included. It also follows that the mass and energy balance in the compartment are explicitly accounted for using this methodology.

4.2.4 Improved Travelling Fire Methodology (iTFM)

The iTFM is a more refined form of the original TFM, aiming to model more credible fire dynamics, by screening out unrealistic fires and introducing the concept of flame flapping angle to account for lower mean near field temperature (see Figure 1). The limitation of the fire size in this method is between 0.2% to 44% of the compartment floor area and is based on the fire spread values used by Clifton in the LFM [22].

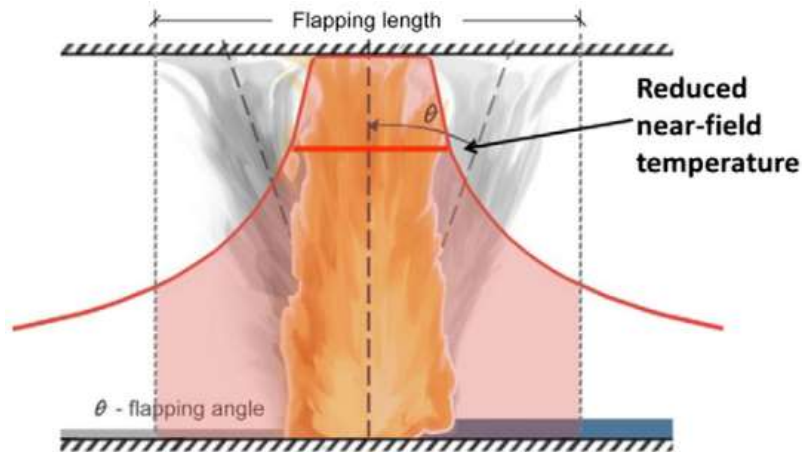


Figure 1 Representation of Flapping Length (f) on the ceiling and angle (θ) [22]

The result is an algebraic expression to obtain the near field temperature as shown below:

$$T_f = T_\infty + \frac{T_{nf}(2r_{x1} + L_f) - 2T_\infty \cdot r_{x2}}{f} + \frac{32.28\dot{Q}^{\frac{2}{3}}}{H \cdot f} (r_2^{1/3} - r_{x2}^{1/3}) \quad \text{Eq. 3 [22]}$$

The Alpert correlation, as outlined in Section 4.2.2 is maintained when calculating the far field temperature due to its simplicity [22].

4.3 TRAVELLING FIRES – PARAMETERS OF INTEREST

4.3.1 Ventilation Openings

The influence of ventilation on the fire development and temperature evolution in small compartments has been well documented in many independent research endeavours ([11] [23] [24][25]). More interestingly, similar studies have been conducted in larger enclosures, identifying more complex fire behaviour. Thomas [26] highlighted in his research that deep enclosures were strongly influenced by ventilation and that non-uniform fires occurred throughout the depth of the enclosure.

4.3.1.1 Size – Ventilation Factor

Large compartment fire tests have shown that the net effect of ventilation is complex and cannot be predicted through manual calculations alone. Some experiments positively correlate to Kawagoe's equation i.e., $\dot{m} = A_o\sqrt{H}$ [27], showing a decrease in HRR and peak temperature in fuel rich conditions as opposed to well ventilation conditions [28][29]. However, in certain tests, it was observed that large opening factors, favouring fuel lean conditions, led to lower peak temperatures [19], presumably due to the venting of hot gases to the outside of the compartment. These competing behaviours should therefore be thoroughly explored.

4.3.1.2 Location of Fire Origin

Experiments conducted by Kirby et al. [4][5], showed that burning behaviour was strongly affected by the position of the seat of the fuel with respect to ventilation opening. In one experiment, the crib at the rear was ignited while the ventilation opening was at the front of the deep enclosure. Figure 2 shows the temperature time evolution inside this enclosure for cribs placed at the rear, middle and front of the compartment.

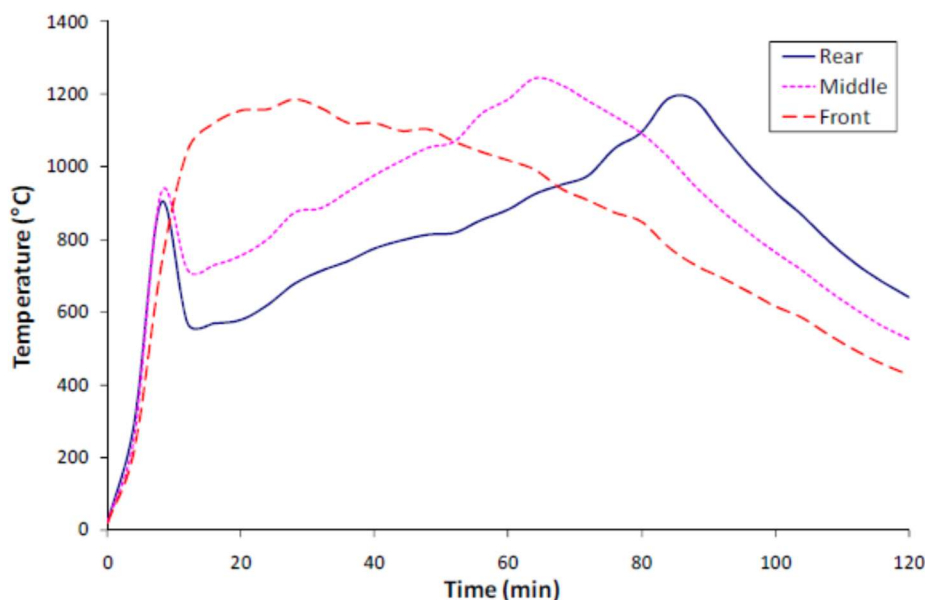


Figure 2 Temperature time evolution at rear, middle and front locations of a long enclosure. [5]

It is apparent that the rear and middle compartments are oxygen starved because of the remoteness of the only ventilation opening as opposed to the front cribs. For these reasons, there are many insights to be drawn from investigating the effect of ventilation size, position, time of opening and symmetry of openings.

4.3.2 Geometry of Compartment

It has been observed that fire spread in long compartments, while initially spreading radially in a two-dimensional fashion, transitions into a one-dimensional fire spread as the compartment walls are reached [30] and the fire spread is limited to only one axis. This phenomenon is illustrated in Figure 3.

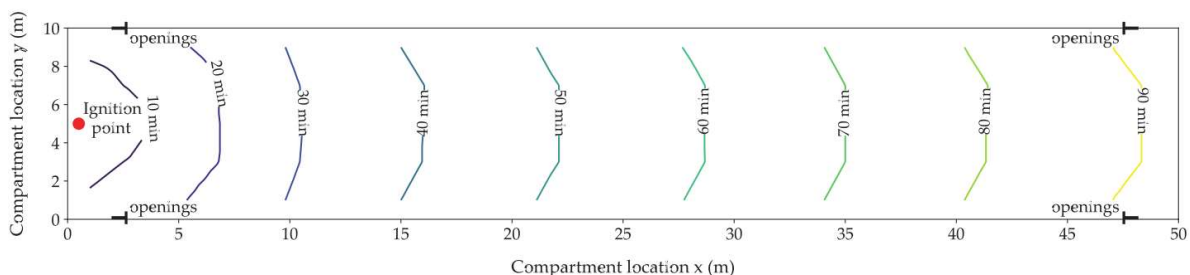


Figure 3 Flame front at different time stamps. Notice the radial flame front within the first 10 minutes transitioning into a more linear fire spread at 30min mark. [30]

It would be interesting to validate how well current travelling fire models can cope with changes in fire spread regime.

4.3.2.1 Height of compartment

A study conducted by Wahlqvist *et al.* [31] has investigated the different characteristics on design fires and showed that higher compartment ceilings typically led to lower HRR. This was attributed to the reduced radiation feedback from the smoke. The authors also commented that in small rooms, most of the radiative feedback emanated from the walls of the enclosure. The variation of compartment height in large enclosures could therefore exhibit a different behaviour due to the decreasing weight of the wall radiation with respect to the smoke layer.

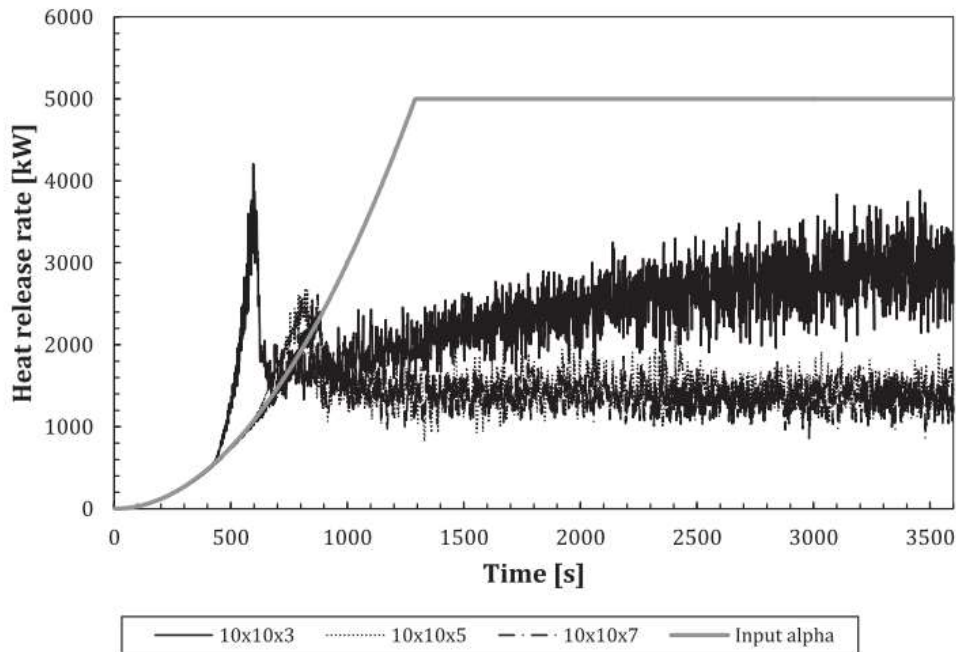


Figure 4 HRR as a function of different ceiling heights (3m, 5m, 7m) [31]

4.3.2.2 Floor Dimensions (Length to Width ratio)

It is expected that the shape and size of the compartment will play a role in the dynamics of the fire spread. It is envisaged that the geometry of room will affect smoke movement and the intensity of radiation feedback. Longer smoke residence times are expected in corridor-like compartments.

4.3.3 Heat Release Rate (HRR)

The choice of HRR is one of the most important properties to consider in fire dynamics. It is known that gas temperature is positively related to the HRR and has been expressed through algebraic expressions [27]. Experiments conducted by Welch *et al.* [19] reiterated that the fuel type is an important parameter to characterise, in the context of fire dynamics study in large compartments. Therefore, information about the HRR of the fuel chosen for experiments is essential in order to identify patterns and logically understand the behaviour of travelling fires. Specification of the fuel should thus be conducted with minimal uncertainty as far as reasonably practicable.

4.4 METHODS OF RESEARCH

4.4.1 Full -Scale Tests

Several full-scale tests have been conducted to further clarify the behaviour of fire in large compartments. These tests, coupled with other analytical methods, have allowed us to grasp the previously poorly understood fire behaviour. However, the cost implications to set up and run full scale experimental setups, especially large fire tests, can be very expensive. This problem is further exacerbated by the fact that, for travelling fire phenomena, a large amount of space, instrumentation and time is required to set up the experiments. As a result, the full-scale experiments are seldom performed and, if attempted, coordinated in such a way to maximise the amount of data and research that can be derived from it.

4.4.2 Reduced Scaled- Experiments

Reduced scaled experiments have positioned themselves as a promising alternative to large scale fire tests due to the reduced space footprint and need for materials. Through a series of validated experiments, Ingason *et al.* [32] have shown very good agreement of the application of the Froude scaling technique to devise reduced scale experiments. Although the research focused on tunnel configurations, it is deemed that larger open plan compartments studied in this thesis possess a similar tunnel-like geometry. The technique could thus be extended to perform reduced scale experiments in future works based on this study. A summary of scaling correlations is provided below.

Table 1 Scaling Correlations

Parameter		Scaling Model	Eq. No.
Heat Release Rate	(kW)	$\frac{\dot{Q}_F}{\dot{Q}_M} = \left(\frac{L_F}{L_M}\right)^{5/2}$	Eq. 4
Volume Flow	(m ³ /s)	$\frac{\dot{V}_F}{\dot{V}_M} = \left(\frac{L_F}{L_M}\right)^{5/2}$	Eq. 5
Velocity	(m/s)	$\frac{u_F}{u_M} = \left(\frac{L_F}{L_M}\right)^{1/2}$	Eq. 6
Time	(s)	$\frac{t_F}{t_M} = \left(\frac{L_F}{L_M}\right)^{1/2}$	Eq. 7
Energy	(kJ)	$\frac{E_F}{E_M} = \left(\frac{L_F}{L_M}\right)^3$	Eq. 8
Mass	(kg)	$\frac{m_F}{m_M} = \left(\frac{L_F}{L_M}\right)^3$	Eq. 9
Temperature	(K)	$T_F = T_M$	Eq. 10

4.4.3 Numerical Study

The surge in computational efficiency and power over the past decades has been a great asset to the development and widespread use of computational fluid dynamics, making numerical study a viable option to consider for research purposes. The advantages of using numerical methods is very well presented in a review by Johansson [33] and are summarised below:

1. Resource efficient – requires much less instrumentation than required for a full-scale test.
2. Much less expensive to run numerical simulations than full-scale experiments.
3. Multiple numerical simulations can be run concurrently unlike large scale tests.
4. Possibility to circumvent the problems associated to scaling.
5. Ability to tackle large geometries which would not be feasible at full scale

The ability to have a high spatial resolution in the context of travelling fires is a significant proponent to the use of numerical methods. The addition of sensors can quickly become a bottleneck in full and reduced scale experimental setups and the lack thereof has often been criticised by researchers [5].

It is noted that there are modelling and uncertainties associated with the use of numerical systems. The assumptions and limitations of the modelling software are considered and dealt in greater detail in Section 5.1.5. Due to the size of the domain and level of accuracy required to predict the temperature within the computational cost can also become prohibitively expensive. The use of high-performance computing can partially alleviate this problem; nevertheless, the exponentially increasing resource cost of simulations at finer mesh size still limits to a large extent the quality of the numerical experiments run. A mesh sensitivity study can be carried out to determine the magnitude of mesh size dependent errors.

4.5 CURRENT LIMITATIONS OF TRAVELLING FIRE RESEARCH

- **Validation of Results**

Due to the significant cost associated with setting up large scale experiments, the validation of travelling fire research is restricted. Numerous large-scale tests highlight the need for several key elements, aside from the funds, to perform such studies. These include the provision of an experimental building to carry out the test, the need for a significant amount of material (combustibles and insulating linings), sensor arrays, as well as firefighting support [34]. The coordination of all necessary stakeholders and items mentioned above contribute to the relatively scarce knowledge base for data validation in large scale compartment fires.

- **Availability of Experimental Results – Lack of spatial resolution**

As highlighted earlier, the ability to measure temperature fluctuations over time at different locations is an essential part of travelling fire study. By extension, the larger the compartment under study, the greater the amount of sensors required to measure the spatial and temporal temperature distribution. For this reason, the lack of spatial resolution is identified as a barrier to travelling fire research.

- **Parameter Sensitivity**

Fires are a highly dynamic and complex process that depends on numerous factors such as material properties, ventilation conditions, compartment geometry and fuel load amongst many others. Therefore, it is quite difficult to characterise with high certainty the way in which a fire would evolve given a set of boundary conditions. As a result, a series of experiments are often required to define the impacts of certain parameters on the fire behaviour. The high cost of travelling fire experiments thus further limits the ability to comprehensively test different parameters thereby restricting the progress in the travelling fire research.

- **Simplification of Fuel Packages**

In order to better characterise the initial conditions of experiments, researchers tend to utilise fuel packages of known fire development characteristics. In this thesis, the same approach is used, allowing for reasonable prediction of HRR of fuel packages. Similarly, the fuel packages are simplified for the purpose of the CFD study. Some travelling fire methodologies assume a homogenous fuel distribution. However, one is reminded that, in real compartment fires, the fuel load is not homogenous and has varying fire interaction characteristics. The results from experiments thus reflect simplified compartments.

5 METHODOLOGY

Since the study being undertaken consists of applying existing methods, running CFD simulations and comparing the results, the algebraic method and CFD simulations are detailed in their respective sections within this chapter.

5.1 FDS MODEL DEVELOPMENT

5.1.1 Fire Dynamics Simulator (FDS) and High-Performance Computing (HPC) Infrastructure

The numerical simulations conducted in this thesis were run using a Large-Eddy Simulation (LES) software for low-speed flows, with an emphasis on smoke and heat transport from fires, called FDS [35]. The HPC Tier 2 infrastructure provided by Vlaams Supercomputer Centrum – Ghent University is used to run the FDS software (version: FDS 6.7.0).

5.1.2 Geometry and Boundary Conditions

In order to capture travelling fire behaviour, it is necessary to design a large computational domain; a compartment of 40m by 10m was constructed in FDS. These dimensions are deemed both large enough for the purpose of the study while maintaining a reasonable amount of computational time to run the simulations. While the default height was set at 4m, this value is modified to investigate the impact of compartment height on fire spread. Openings are provided on both sides of the longer facades to allow for influx of fresh air. It should be noted that the openings are set at a height representative of typical windows. The opening does not extend to the ceiling thereby allowing a smoke layer to be built up. The computational domain around the openings is extended to minimize air flow errors caused by the pressure solver at the mesh boundary. Detailed dimensions of the compartment are presented in Appendix 10.1.

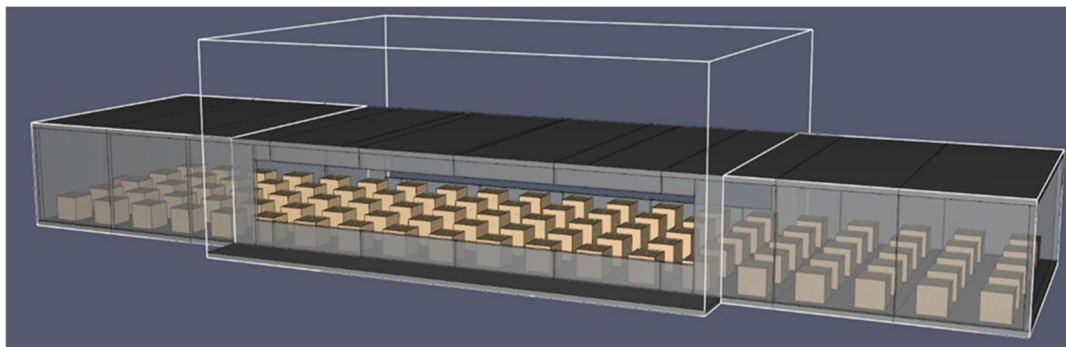


Figure 5 FDS Visualisation of Cribs in Open Plan Compartment

Owing to the size of the computational domain, it was important to evenly distribute the computational load over the number of cores used to run the simulations. A diagnostic simulation was run to identify the smoke travel path upon exiting the compartment and it was observed that the smoke seldom spread over the roof but rather spilled further horizontally upon exiting the compartment, after which it was transported vertically. The computational boundaries were adjusted to avoid clipping the smoke too close to the compartment openings. Further details on the mesh boundary is provided in Appendix 10.3. The material properties of the boundary walls, floor and ceiling were assumed to be those of concrete. The wooden cribs were assumed to bear the same material properties as those of pine wood. The values used are summarised in Table 2.

Table 2 Material Properties used in CFD simulation

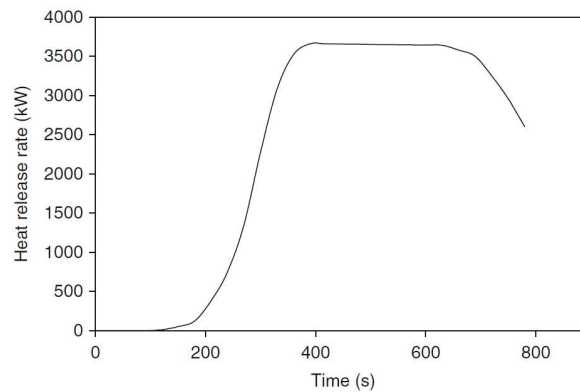
		PROPERTIES			SOURCE
		k	ρ	c	
MATERIAL		$W/m \cdot K$	kg/m^3	$J/kg \cdot K$	
Walls	Concrete	1.1	2100	880	[27]
Floor	Concrete	1.1	2100	880	[27]
Ceiling	Concrete	1.1	2100	880	[27]
Fuel Package	Yellow Pine	0.147	640	2800	[17]
Burnt out package	Yellow Pine	0.147	640	2800	[17]

5.1.3 Fire Characteristics

It is especially important to characterise the fire source to allow for both accurate numerical simulations and validation through subsequent reduced scaled experiments. For this reason, the fuel packages are modelled based on research available on wooden pallets. This choice is supported by the following reasons:

1. Availability of the HRR curve from experimental data.
2. Generalised equation for prediction of peak HRR for a range of wood pallet sizes.
3. Availability of validated scaling experiments using wooden pallets.

The heat release rate of a typical wooden pallet stack (1.22 x1.22 x1.22m) is illustrated in Figure 6. It is of interest to observe that that a plateau in HRR is achieved, similar to burning wooden crib behaviour as noted by Babrauskas [36]. It is noted that Babrauskas derived these results using a furniture calorimeter are more similar to an open burning scenario rather than an enclosed space burning behaviour.


Figure 6 Heat Release Rate curve for a typical wooden pallet fire (1.22 x 1.22 x 1.22m) [17]

The SFPE Handbook also provides a generalised formula expressing the maximum HRR, i.e., the plateau in Figure 6 in terms of stack height and moisture content. The equations are presented below.

$$\dot{q} = 1368(1 + 2.14h_p) \times (1 - 0.03M), \text{ for standard pallets} \quad \text{Eq. 11 [17]}$$

$$\dot{q} = 919(1 + 2.14h_p) \times (1 - 0.03M), \text{ for non - standard pallets} \quad \text{Eq. 12 [17]}$$

Where h_p = stack height (m)

M = moisture content (%)

The equation allows the calculation of preheated and subsequently drier fuel packages in addition to those maintained under normal conditions. While the preheating is not modelled in this study, the above equations could be used for such purposes in future works.

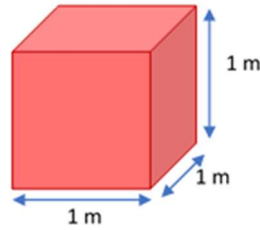


Figure 7 Individual Fuel Package Dimensions

The top and side faces only ignite and contribute to fire spread. This is equivalent to a maximum of $1 \times 5 = 5\text{m}^2$ of burning area per fuel package. The bottom face, in contact with the floor, does not burn.

The wooden pallets are modelled in FDS using 1m cubes with an initial moisture content of 5%. It is assumed that the HRR curve shown in Figure 6 is representative of the HRR evolution irrespective of the peak HRR value and is thus scaled to match the calculated peak HRR.

The peak HRR is thus calculated as follows from Equation 12:

$$\dot{q}_{peak} = 919(1 + 2.14h_p) \times (1 - 0.03M) = 919(1 + (2.14 \times 1.0)) \times (1 - 0.03(5)) \approx 2453 \text{ KW}$$

For one fuel package, the exposed area available for flame spread is 5m^2 ; the corresponding HRR per unit area of fuel package surface is therefore 490.6 KW/m^2 . The growth and decay of the fuel package is determined by digitizing the HRR curve from experiments illustrated in Figure 6. The obtained values are then used to generate the HRR ramp in FDS. The FDS code can be found in Appendix 10.4.

5.1.4 Fire Spread Modelling

Given that travelling fires are characterised by a moving flame front, the rate of fire spread is a key phenomenon requiring due consideration. However, fire spread is dependent on several variables such as HRR and material properties of the fuel. Due to the lack of available data, it has proved difficult to determine the aforementioned properties, leading to poor predictions of fire spread [37]. Studies conducted by Yuen *et al.* [38] have shown that change in temperatures affect the material composition and hence the pyrolysis process, which is itself strongly linked to fire spread. Bearing this in mind, the fire spread is modelled dynamically in FDS to provide a realistic realisation of the fire growth and temperature profile within the compartment. Initially, the critical heat flux or critical temperature for ignition were proposed as potential triggers for flame propagation onto discrete fuel packages in FDS. However, research conducted by Vermesi *et al.* [39] have concluded that irradiation alone is not a reliable predictor of wood ignition. The critical temperature for ignition of wood was therefore used as the parameter for flame spread between fuel packages. This reasoning was supported by the findings from Yudong *et al.* [40] stating that using temperature of the order of 300°C will give conservative results in simple heat transfer models of ignition. Using this approach, each fuel package is assigned an ignition temperature of 300°C and ignites automatically once the temperature of the fuel packages' surface reaches this assigned value.

The advantage of this approach is that radiation from multiple sources is accounted for in the fire spread, thus providing more realistic fire propagation. It should however be kept in mind that this approach is reliant upon the quality of the resolution of the temperature profile; a fine mesh is required to obtain reasonably accurate results. Additionally, because FDS uses a discretized form of the radiation transport equation (RTE) utilizing solid angles [41], the quality of radiation modelling will drop very rapidly as distance between the emitting and receiving body is increased. The non-uniform

distribution of the radiant energy due to this discretization, called the 'ray effect', will lead to hotspots thereby decreasing the quality of the simulation. For this reason, the fuel packages are spaced at relatively small intervals of 1 metre in all the simulations run.

5.1.5 Mesh Treatment

One of the main challenges posed by this study was the size of the compartment to be studied from a numerical analysis standpoint. Travelling fires are associated with large compartments where localised flashovers progress through the enclosure; the effect cannot be replicated in smaller compartments because the flashover leads directly to a fully involved room. Therefore, it was important to characterise an enclosure of dimensions that would allow the travelling fire phenomenon to be observed while not increasing unnecessarily the size of the computational domain. The dimensions used in the numerical study were informed by the above-mentioned reasoning. Moreover, all simulations were run using the High-Performance Computing (HPC) Infrastructure of Ghent University which provided the ability to running the simulations on multiple threads in parallel. For this reason, most simulations were broken down into multiple meshes and run to reduce the compute time 16-fold (16 to 20 threads used). It should be noted that the mesh boundaries were situated as far as possible from the burning surfaces modelled to minimise the risk of numerical instabilities.

5.1.5.1 Turbulent Flow Scales

It is essential that the turbulent eddies of the simulation are resolved to a sufficiently fine scale to avoid introducing modelling errors. A too coarse mesh will cause large eddies in the energy-containing range, still geometry dependent, to be modelled instead of being resolved. To ensure the mesh size falls within the universal equilibrium range where the eddies are considered to be isotropic, the characteristic length scale of the inertial subrange is defined.

Based on Pope [42], typically, the onset of the inertial subrange is defined as:

$$l_{EI} = \frac{l_o}{6}$$

Where l_{EI} is the inertial subrange length scale

l_o is the length scale of the geometry.

In order to be conservative, the geometry length scale is assumed to be smallest value of the model geometry, i.e., the height of the compartment. In this case, the lowest compartment height studied was at 3 metres.

The l_{EI} length scale is calculated to be $l_{EI} = \frac{3}{6} = 0.5\text{m}$. This value provides an indication of the maximum mesh size that will not introduce significant modelling errors from a perspective of capturing turbulent energies. Based on the above assessment, mesh sizes smaller than 0.5m are considered for further investigation.

5.1.5.2 Non-Dimensional Fire Diameter and Plume Resolution Index

The FDS User Guide provided some guidelines on how to treat mesh resolution. A measure of how well the flow field is resolved can be gauged by determining the Plume Resolution Index (PRI), which is the ratio of the characteristic fire diameter over the mesh spacing.

The dimensionless fire diameter and PRI are expressed as follows:

$$D^* = \left(\frac{\dot{Q}}{\rho_\infty c_p T_\infty \sqrt{g}} \right)^{\frac{2}{5}}$$

$$PRI = \frac{D^*}{\delta x}$$

Where δx is the mesh filter size.

In most experimental setups, the FDS validation guide reported values for the $D^*/\delta x$ ratio between 5 and 15 [41]. Based on the design fire characteristics, the corresponding values are calculated for $D^*/\delta x$ and summarized below. The heat release rate \dot{Q} , was taken to be that of a fully involved row of fuel packages since it was deemed to be representative of the average fire size within the compartment.

$$D^* = \left(\frac{12265}{1.204 \times 1.005 \times 293 \times \sqrt{9.81}} \right)^{\frac{2}{5}} = 2.614$$

Table 3 shows the calculated values for mesh sizes tried during these simulations.

	Very Coarse	Coarse	Moderate	Fine	Fine
Mesh size, m	0.5	0.4	0.2	0.1	0.05
$D^*/\delta x$	5.23	6.54	13.07	26.14	52.28

While the results presented in the above table do not provide a definitive idea of the quality of the results, they provide an indication of potentially adequate meshes sizes that can be utilised for the simulations. Therefore, based on the PRI, mesh sizes of 0.2m, 0.1m and 0.05m were considered for further study.

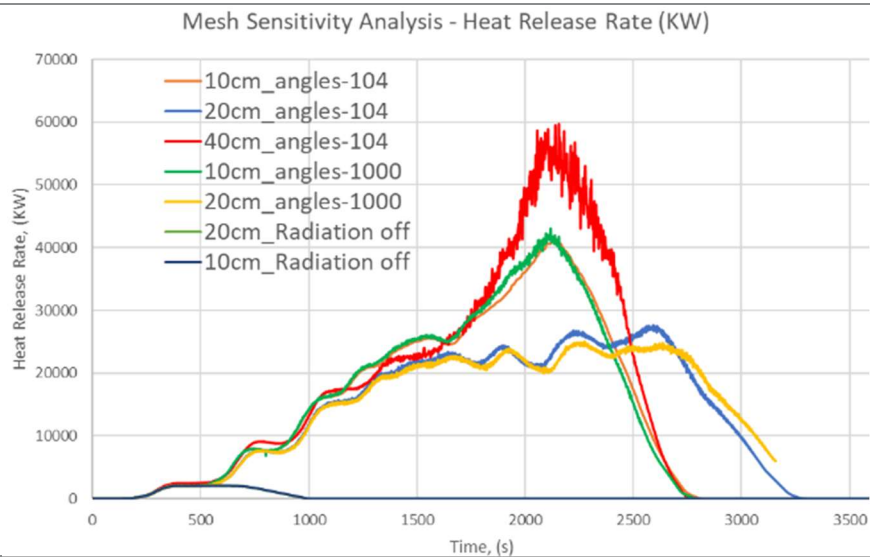
5.1.5.3 Mesh Sensitivity Study

A mesh sensitivity analysis is carried to determine the most representative results at reasonable computational cost. The initial approach employed was to run simulations on gradually finer meshes until no appreciable differences in the parameters being sought were obtained. However, it was also important to consider the computational power available and corresponding time required. A preliminary analysis showed that the computational time of the 0.1m mesh was of the order of weeks. To save on the computational time, the mesh sensitivity study was carried out on a portion of the domain, i.e., the first 20m of the compartment, which effectively reduced the computational time by roughly half. The table below summarises the time taken to run the simulations using the HPC infrastructure (excluding queuing time) and emphasises the limitations of refining the mesh to 0.1m and lower. The geometry details can be found in Appendix 10.4.

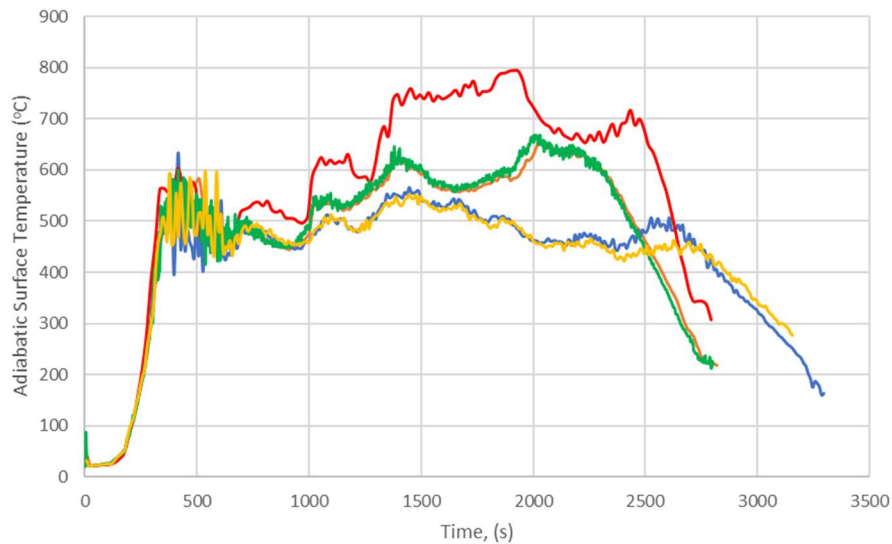
	Coarse	Moderate	Fine	Fine
Mesh size, m	0.4	0.2	0.1	0.05
Number of Cells	12500	100,000	800,000	6,400,000
Computational Time	6-7hrs	48-72hrs	9-12 days	N/A
$D^*/\delta x$	6.54	13.07	26.14	52.28

Table 4 stresses the expensive computational times associated with meshes smaller than 0.2m. Since the simulations in this study are roughly twice as larger as those run for the mesh sensitivity study, it can be inferred that the run time for a 0.1m simulation would require in excess of a month. These results therefore place significant limits to the ability to resolve the fire dynamics at a finer mesh scale given the timeframe available for this study. The results obtained for different meshes and different number of radiation angles are compared and presented in Table 5.

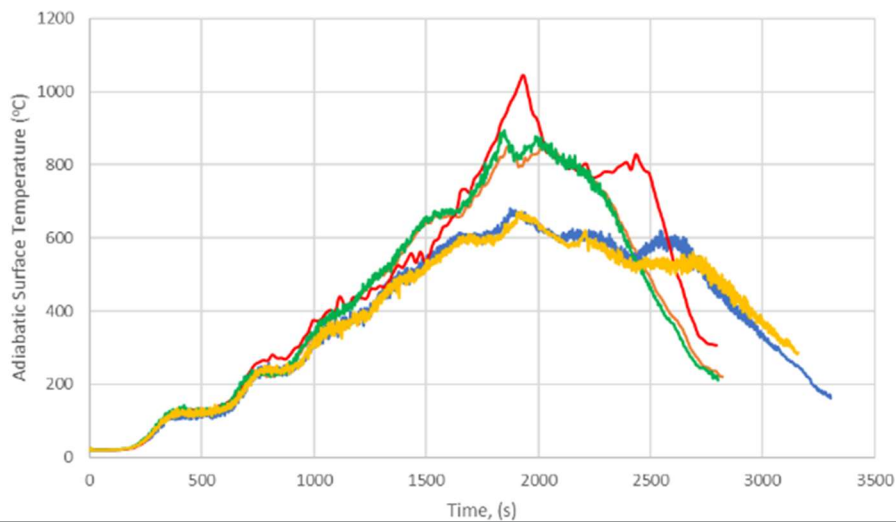
Table 5 Mesh Sensitivity Study - Comparison of Adiabatic Ceiling Temperatures and Heat Release Rates



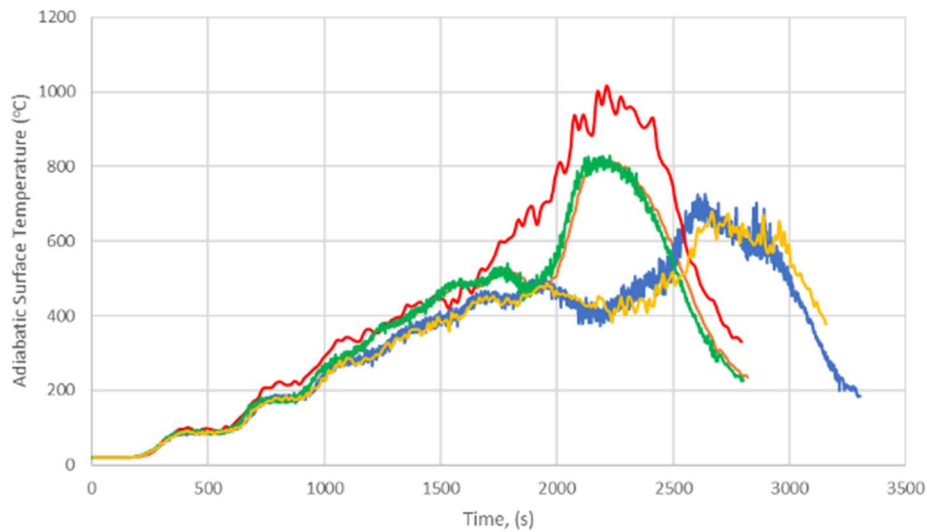
Mesh Sensitivity Analysis - Adiabatic Surface Temperature (°C) at position (0.9,5.0)



Mesh Sensitivity Analysis - Adiabatic Surface Temperature (°C) at position (6.9,5.0)



Mesh Sensitivity Analysis - Adiabatic Surface Temperature (°C) at position (14.9,5.0)



From the results, it can be inferred that mesh convergence for HRR and ceiling temperatures are not achieved with 0.4m and 0.2m meshes. The 40cm mesh leads to a significant overprediction of the HRR in the simulation subsequently causing more elevated temperatures to be recorded at the ceiling level in all positions within the compartment. The opposite is observed for the 20cm mesh, whereby underpredictions in temperature are recorded when compared to the 10cm mesh. It is also noted that the divergence in results occur after 1600s of burning, where the discrepancy in HRR between the different mesh sizes amplify the difference between the measured temperatures. Based on these results, it can be inferred that the inaccuracies in predicting the temperatures within the compartment become increasingly apparent as time progresses in the simulation. This highlights a potential limitation of the fire modelling approach employed; the heat feedback is responsible for flame spread in the simulations and subsequently, deviations are magnified as the fire event progresses.

Given that the flame spread and HRR is associated with the temperature exposure of the fuel packages, overpredictions (e.g. 40cm mesh) or underpredictions (e.g. 20cm mesh) of temperature in the compartment lead to increasingly divergent behaviour as the fire develops. These findings stress the need to run the simulations on very fine meshes in order to capture the fire spread correctly. A further step would be to validate the simulations against reduced scaled experiments to improve the accuracy of the results.

While it is acknowledged that the 20cm mesh cannot provide accurate temperature predictions, it is used during the course of this thesis because it still gives an indication of the temperature-time trends observed in travelling fires. Furthermore, the main reason for not employing a 10cm mesh is the computational time required. Additionally, the quality of the 10cm mesh cannot be guaranteed without validation through experiments thereby stressing the need to support such simulations in future studies with experiments. It is still strongly recommended that this study be conducted on a finer mesh in further work until mesh convergence is achieved especially if temperature exposure is of interest.

Another important characteristic of the simulation is the modelling of the radiation. The radiation solver accounts for about 30% of the computational time; for this reason, different number of radiation angles were investigated to identify their impact on the results [43]. When no radiation was modelled, flame propagation did not occur at neither 20cm nor 10cm mesh size, as can be observed

in Table 5, thereby emphasizing that radiation plays a crucial role in the fire spread inside the compartment despite 65% of the HRR being released through convection. Based on these findings, it was deemed that radiation modelling could not be ignored in subsequent simulations. The quality of the radiation modelling was investigated by increasing the number of radiation angles and comparing the results. It was concluded that increasing the number of radiation angles did not appreciably increase the quality of the simulations at the mesh sizes studied. It can be inferred from the results that for mesh sizes of 10cm and higher, the mesh is already saturated with 104 radiation angles. Therefore, increasing the radiation angles for such mesh sizes only increases the computational cost but does not yield improved results. A higher number of radiation angles should however be attempted if a finer mesh (e.g. 0.05m or 0.01m) or if a larger spacing within fuel packages is utilised in further research. Based on the findings, the simulations were run using a 20cm mesh with 104 radiation rays.

Values of the incident heat flux at different radiation angles were also compared and are presented in Figure 8. In a similar vein to results observed for the temperature profiles, it can be concluded that the number of radiation angles have marginal impact on the quality of the results. Nevertheless, the results show that the heat flux is severely underpredicted by the 20cm mesh; the peak heat fluxes differ by 45% between the two cases. Due to this larger uncertainty, the use of heat flux measurements is only used as an indicative tool in this study.

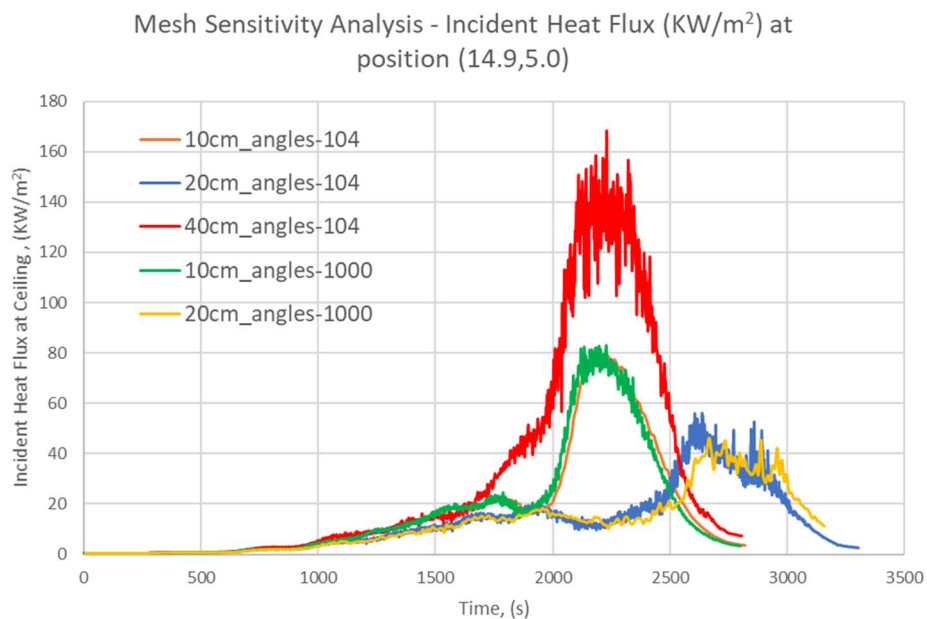


Figure 8 Comparison of Incident Heat Flux for different mesh sizes and radiation angles

5.1.6 Simulation Input Parameters

The simulation input parameters coded into the FDS codes are presented in this section. The detailed dimensions, FDS code, and HPC script are presented in Appendix 10.1, 10.5, 10.6 respectively.

5.1.6.1 Case 0 - Control Case

The control case is modelled to represent an array of fuel packages in a large open plan rectangular compartment. The fuel packages are distributed evenly throughout the compartment to replicate a uniform fuel load density across the whole floor area. The compartment consists of 20 rows of 5 sets of stacks amounting to a total of 100 stacks as shown in Figure 9. The distance between two adjacent fuel packages is fixed at one metre in order to minimize the error associated to radiation propagation in FDS. Openings were provided on both sides of the longer faces of the compartment. Graphs presented in this document will utilize the coordinates system illustrated below.

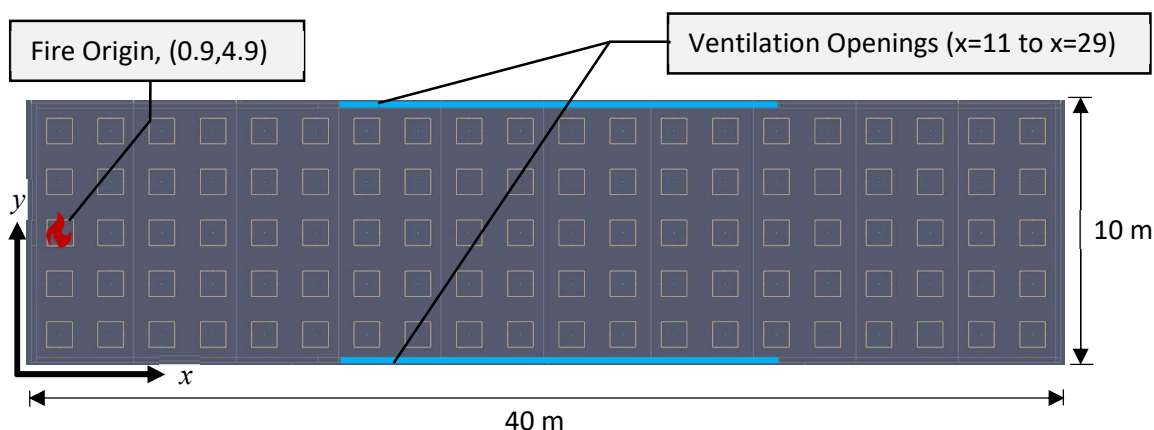


Figure 9 Plan view of compartment showing arrangement of fuel packages

5.1.6.2 Case 1 – Increased Ventilation

In case 1, the general layout of case 0 is conserved with the exception of an increased opening area. This was achieved by increasing the height of the opening while maintaining the same clearance from the ceiling and is illustrated in Figure 10 and Figure 11.

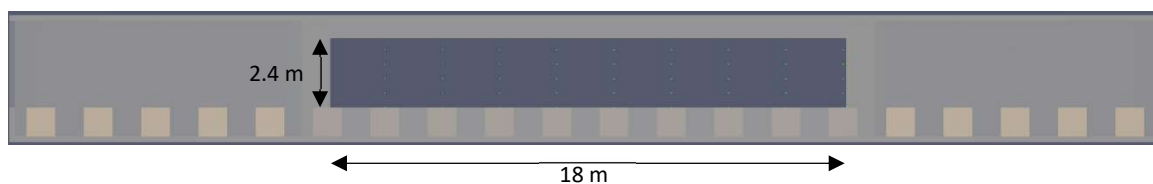


Figure 10 Front View of Case 0 - 18m x 2.4m opening

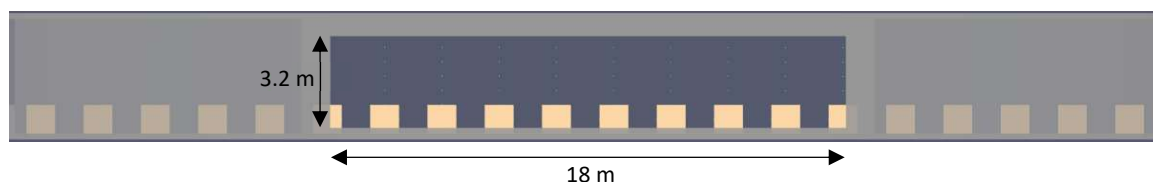


Figure 11 Front View of Case 1 - 18m x 3.2m opening

The objective was to investigate the fire behaviour in varying ventilation conditions as it is expected that the air flow through the openings will affect the flame propagation. The ventilation factor is used to quantify the difference in ventilation; the calculations are presented below.

$$\text{Ventilation Factor, } v_{f,i} = A_o \sqrt{H_o} \quad \text{Eq. 13}$$

$$A_o = \sum_{i=1}^n A_i = \sum_{i=1}^n b_i h_i \quad \text{Eq. 14}$$

$$H_o = \sum_{i=1}^n H_i = \frac{\sum_{i=1}^n A_i h_i}{A_o} \quad \text{Eq. 15}$$

where A_o is the total opening area

H_o is the height of the opening

Applying Equations Eq. 13, Eq. 14, and Eq. 15, the ventilation factors for both cases are calculated below.

$$v_{f,case\ 0} = (2 \times 2.4 \times 18) \cdot \sqrt{2.4} \approx 133.9$$

$$v_{f,case\ 1} = (2 \times 2.4 \times 18) \cdot \sqrt{3.2} \approx 206.1$$

The change in ventilation factor between the two cases is calculated to be 34%.

5.1.6.3 Case 2 – Single Opening

In this case, the ventilation is reduced compared to the base scenario. One opening is removed leading to an asymmetrical ventilation scenario. It is expected that the more significant smoke depth would affect the flame spread through the compartment.

5.1.6.4 Case 3 – Ventilation opening on 2 shorter faces

As documented in previous experiments, the placement of openings at opposite ends of the compartment were shown to affect fire spread behaviour. This case attempts to visualise the temperature profile within the room when subjected to a different opening configuration. Figure 12 shows the placement of the openings leading to a tunnel-like situation. It should be noted that the ventilation factor remains unchanged from the control case, i.e., size and height of openings are the same.

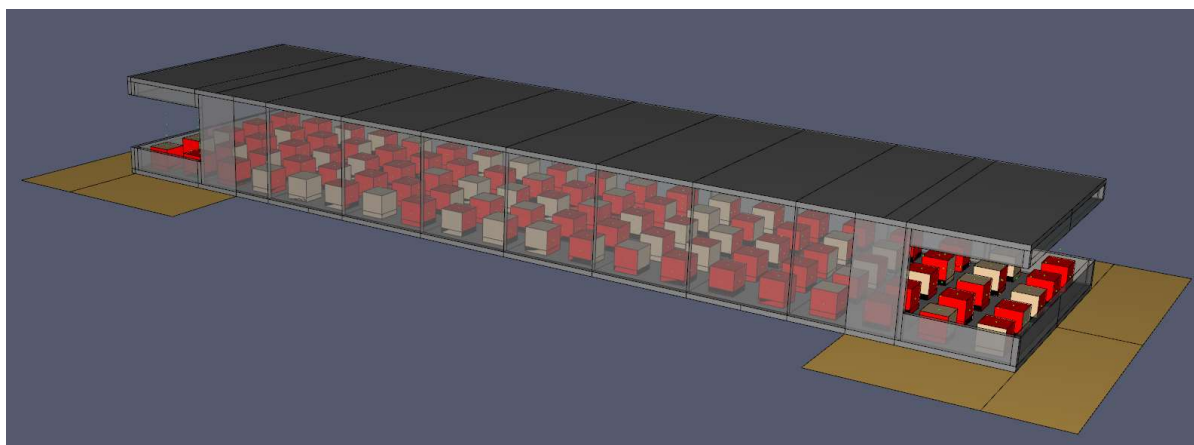


Figure 12 Illustration of model with openings positioned at opposite ends of the compartment

5.1.6.5 Case 4 – Lower Compartment Height

The lower compartment height aims to explore the potential impact of increased smoke radiation feedback and flame impingement at ceiling and their subsequent contribution to flame spread to fuel

packages. This is achieved by decreasing the ceiling height to 3m while maintaining the same opening size and ventilation factor as the control case.

5.1.6.6 Case 5 – Increased Compartment Height

Modelling a higher compartment ceiling aims to investigate the effect of a larger smoke reservoir and its subsequent impact on the predictive capabilities of the established travelling fire methodologies. The ceiling is raised to 5m height in this case and the results are then compared.

5.1.6.7 Case 6 – Changing Ventilation Conditions during fire progress

In real fire scenarios, it is highly likely that ventilation conditions evolve over the course of the fire. For this reason, a numerical simulation has been set up to probe the influence of changing ventilation conditions during the fire. A reasonable scenario, involving window breakage at a given temperature is proposed. The windows are set to break at 340°C based on values found in literature [44].

5.1.6.8 Case 7 – Increased Heat Release Rate per Unit Area (HRRPUA)

The increased fuel load density is also examined and compared to the predictions of travelling fire methodologies. Case 7 provides further information on the possible limitations associated with the identified travelling fire calculations. The HRR of each fuel package is increased from the initial value of 2453kW to 4000kW which equates to a change of about 40%.

5.1.6.9 Case 8 – Square Compartment

The effects of physical boundaries altering flame spread is assessed in this scenario. The results could indicate whether the use of travelling fire methodologies can be extended to complex building arrangements (e.g. non-rectangular compartments). The same number of fuel packages are used as in the control case. Similarly, the same ventilation dimensions are maintained.

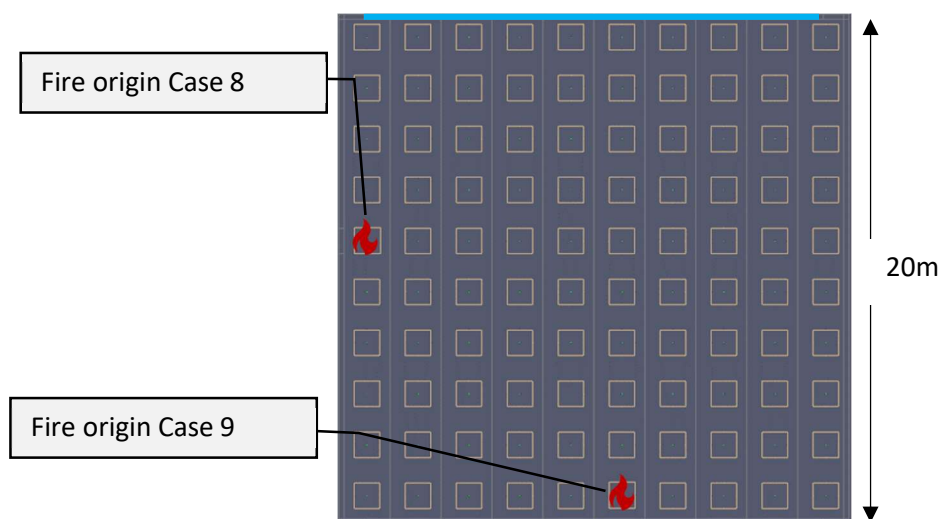


Figure 13 Plan view of square compartment showing arrangement of fuel packages

5.1.6.10 Case 9 – Changing location of fire origin

The same compartment geometry as in Case 8 is used but the fire origin location is moved closer to the openings. The objective of this simulation is to identify fire behaviour changes based on the ignition location.

The first challenge when using this equation was to adapt the formula, which assumes a continuous and uniform fuel load density across the floor plate, to one that consists of discrete fuel packages. In order to circumvent this limitation, the compartment is divided in 10 arrays of 10 fuel packages each and is illustrated in Figure 15. By discretizing the floor plate, an adjusted fuel load density can then be calculated. The green arrow shows the direction of travel of the fire, as it progresses from one array to the next.

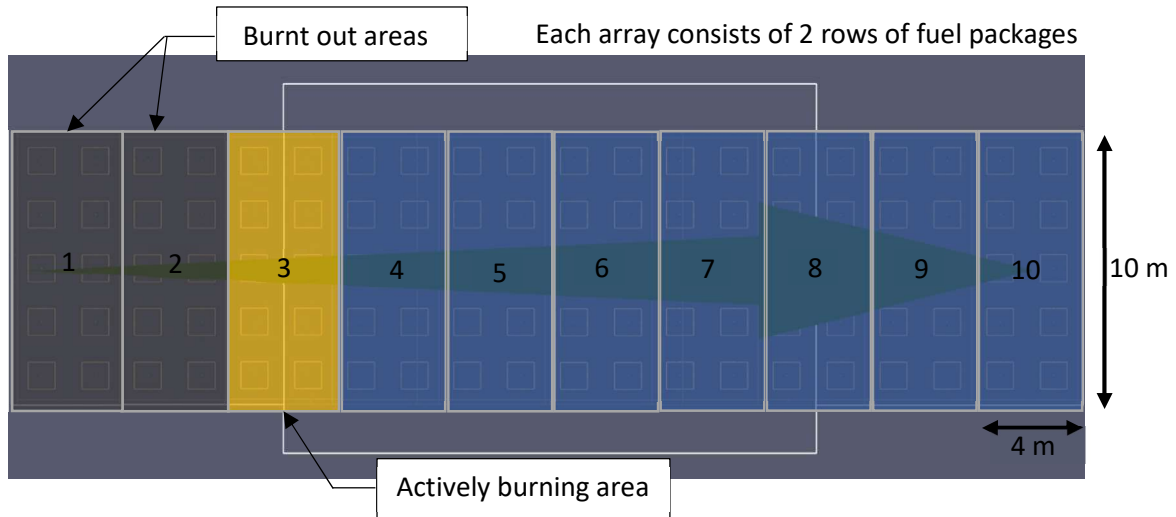


Figure 15 Division of floor plate into discrete sections of uniform fuel load density

However, since the method also assumes a constant HRR per unit area (HRRPUA), it was necessary to establish a representative point value HRR, based on the HRR curve of fuel packages being modelled. This is achieved by quantifying the energy released by the fuel package and averaging the value of the burning time of the package. The energy content of each fuel package is obtained by evaluating the area under the graph of the HRR vs time plot (see Figure 16), using the Simpson's rule.

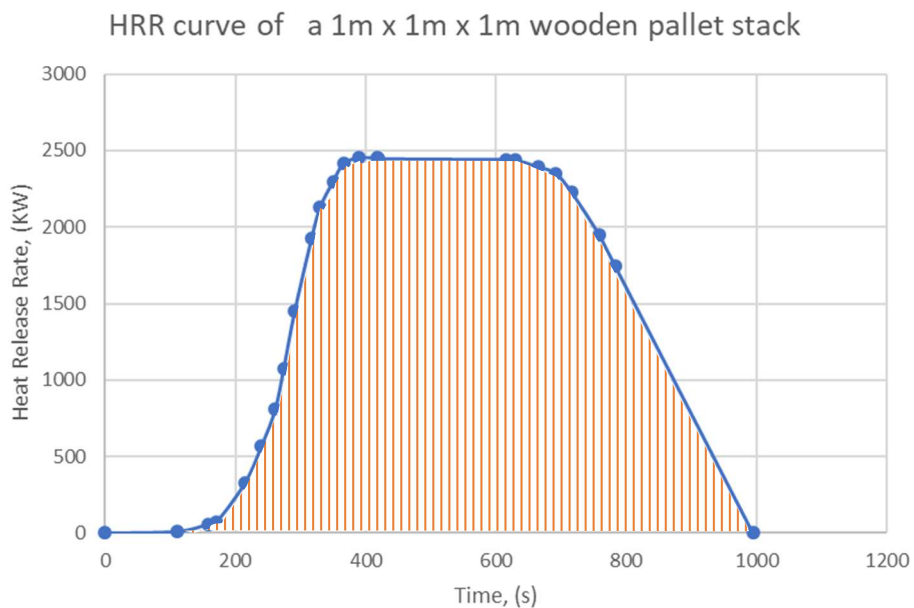


Figure 16 Area under graph showing energy released by fuel package

Using Simpson's Rule

$$\text{Area under Graph, } E = \sum_i^{995} \frac{1}{2} (HRR_i + HRR_{i+1}) \times t_{\text{increment}} = 1360.4 \text{ MJ} \quad \text{Eq. 17}$$

Logically, the total energy released by one array of 40m², consisting of 10 fuel packages would be 13604MJ. The adjusted fuel load density can thus be calculated as 13604/40 = 340MJ/m². Similarly, the HRR per unit area (HRRPUA) is obtained as follows:

$$HRRPUA_{\text{adjusted}} = \frac{E_{\text{total,1 array}}}{t_{\text{burnout}} \times A_{\text{array}}} = \frac{13604}{995 \times 40} = 341.8 \text{ KW/m}^2 \quad \text{Eq. 18}$$

With both the fuel load density and HRRPUA being quantified as point values, it is now possible to determine, using Equation Eq. 16, the predicted temperature at a given point. It should, however, be noted that the temperature is related to the position of the fire, characterised by the value \dot{x}_t . The method uses a constant fire spread rate in order to track the position of the fire within the compartment as shown in Equation Eq. 19. Once again, it is necessary to determine a fixed fire spread value due to the limitations of the methodology.

$$\dot{x}_t = s \times t \quad \text{Eq. 19}$$

Where \dot{x}_t = location of the leading edge of the fire relative to place of fire origin, (m)

s = fire spread rate, (m/s)

t = time since ignition of fuel, (s)

Due to the scarce information on fire spread rates of travelling fires, there is a large uncertainty band associated with this parameter. Values from literature, derived from real building fire investigation reports, include fire spread rates ranging from 1.5mm/s to 19.3mm/s [47]. Two approaches are proposed to tackle this problem. In the first approach, the average fire spread rate is calculated from the numerical simulations and is then utilised to determine \dot{x}_t and then compare the TFM with the numerical results. The second method, is to use the average fire spread rate obtained from literature, i.e., $\frac{1.5+19.3}{2} = 10.4 \text{ mm/s}$. This second option, however, assumes that a blanket single fire spread rate is used for all cases. It is acknowledged that the first option offers limited value to applied fire engineering because of their reliance on the numerical results as an input to the TFM method. However, in this study, the TFM is used as a comparative tool rather than a predictive one. Thus, the use of simulation results to inform the values used in the TFM are deemed acceptable.

6 RESULTS AND DISCUSSION

The results and discussion are presented in three parts. The first part consists of understanding the fire dynamics occurring during a travelling fire event. Secondly, the travelling fire methodology is applied to the results obtained from the numerical simulation and the observations discussed. Finally, the assumption of fixed fire spread is analysed and discussed.

6.1 ANALYSIS OF TRAVELLING FIRE BEHAVIOUR

The temperature time profiles are presented for multiple locations at ceiling level. The locations most referred to are shown in the figure below.

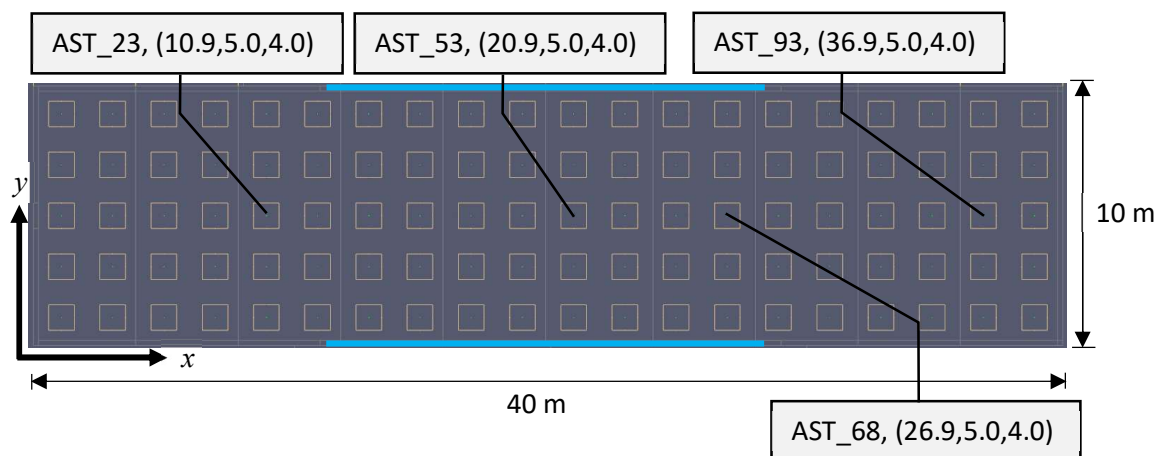


Figure 17 Location of devices measuring temperature profiles in simulations

6.1.1 Control Case - Temperature Profile

The graph below shows the temperature variation over time at four discrete locations at ceiling level in the compartment for the control case.

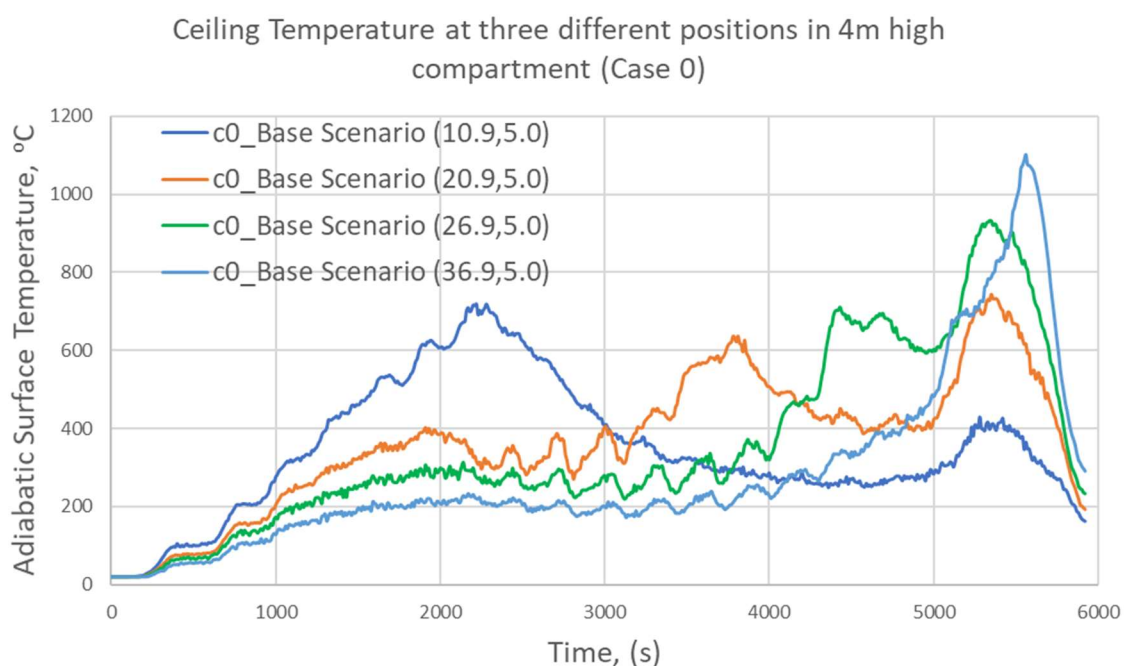
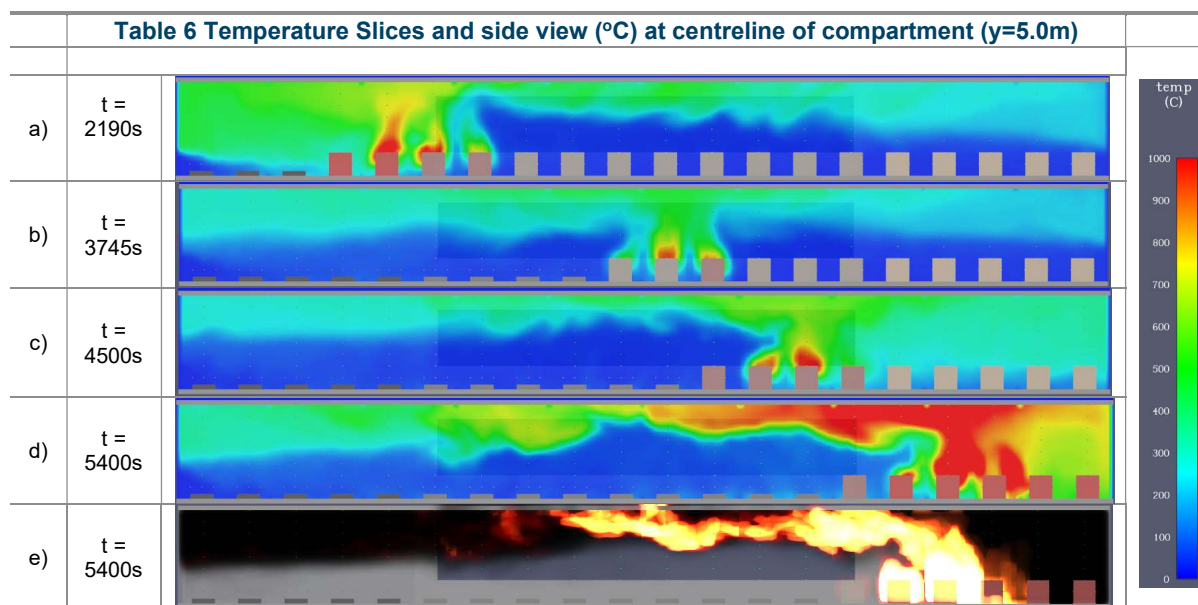


Figure 18 Temperature-Time profile of ceiling at three different positions inside the large compartment for Case 0

It can be observed that the temperature exposure at 10.9, 20.9, 26.9 and 36.9m correspond to travelling fire behaviour; the further the measuring point with respect to the fire origin, the longer the time until the first peak temperature is observed. This initial peak corresponds to the time at which the flame is directly below the measurement device and is confirmed by observing the temperature slices at their corresponding times as shown in Table 6. The slices also reveal that a significant amount of smoke is built up behind the flame front during the first 2200s, leading to a higher temperature (700-800°C) registered by the measuring device. During this period, the smoke is trapped between the walls of the compartment and the flame front, unable to escape effectively through the openings. This contrasts with the temperature slice at 3745s, where a cooler smoke layer (500-600°C) is present. It is also reflected in the 20.9m temperature profile in Figure 18, where the temperature is generally lower than both the 10.9m and 26.9m profiles as smoke can freely escape as well as mix with entrained fresh air.



An interesting behaviour is observed as the flame front progresses past the openings. Once again, the venting of hot smoke is inhibited by the presence of the advancing flame front towards the far end of the compartment. A similar smoke build-up to what occurred in the initial 2000 s of the fire. However, the main distinction in this case, is the presence of unburnt fuel packages at the location of smoke build up (see Table 6 c)). The hot smoke layer descends and thus causes a rapid ignition of all remaining fuel packages located at the far end of the compartment. In other words, the travelling fire behaviour transitions to a traditional flashover event at the end of the compartment.

The localised flashover observed at the end of the compartment leads to a sudden increase in temperature at the ceiling directly above the fuel packages as illustrated in Figure 18 (see 36.9m plot). Due to an oxygen vitiated environment at the end of the compartment, flaming also occurs along the length of the ceiling leading up to the openings. The temperature slice at 5400s confirms the presence of temperatures of 1000°C extending to a large part of the ceiling in the second half of the compartment (i.e., 20m < x < 40m). The flashover prior to complete burnout of the compartment causes a second large spike in temperature as observed in Figure 18. The effect is more prominent at the locations closer to the end of the compartment and suggests that any element at ceiling level may be subjected to elevated temperatures multiple times during a fire in a large compartment. The localised flashover will be of critical importance when comparing the predicted temperature profile from calculations with observations made thus far and is discussed in Chapter 6.4.

6.1.2 Ventilation Opening Configurations

The five different ventilation configurations highlighted in the methodology section are compared. Firstly, Figure 19, Figure 20 & Figure 21, all show that the travelling fire behaviour is present in all ventilation configurations simulated. However, different peak temperatures and burn out times are observed. The legend in Figure 19 also applies to Figure 20 & Figure 21.

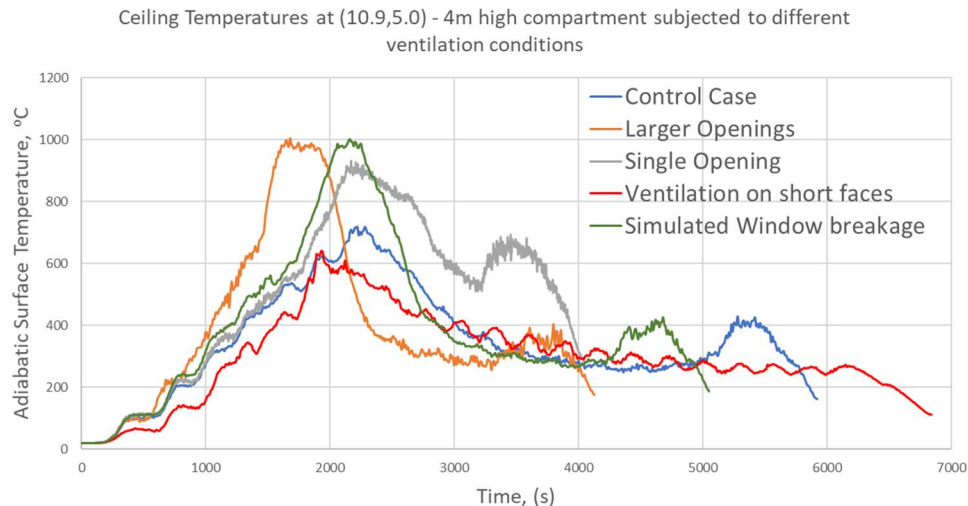


Figure 19 Temperature-Time Profile for different ventilation conditions at (10.9,5.0)
Ceiling Temperatures at (20.9,5.0) - 4m high compartment subjected to different ventilation conditions

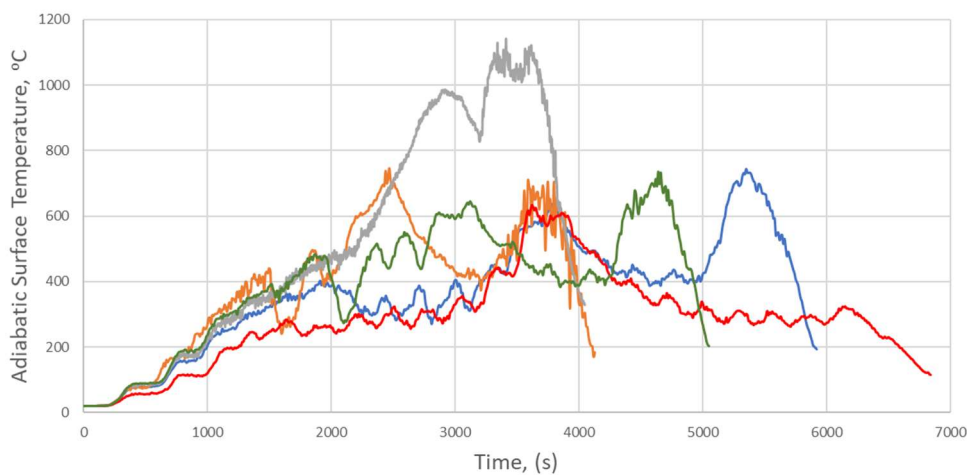


Figure 20 Temperature-Time Profile for different ventilation conditions at (20.9,5.0)
Ceiling Temperatures at (26.9,5.0) - 4m high compartment subjected to different ventilation conditions

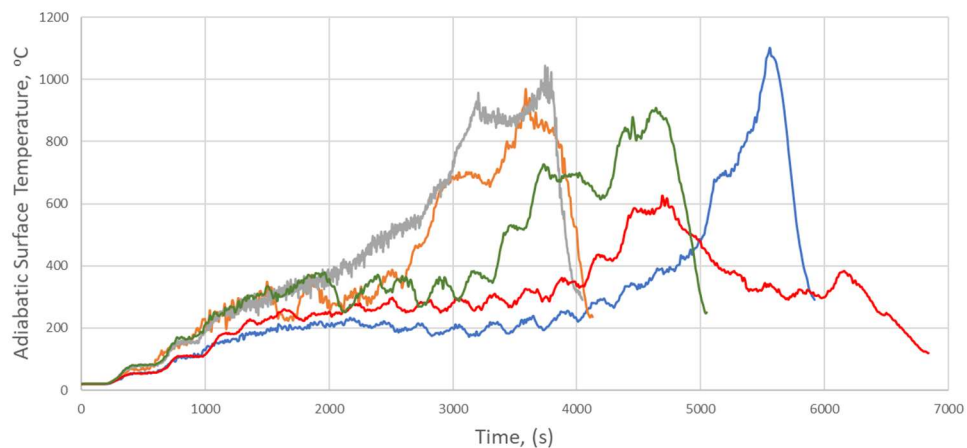
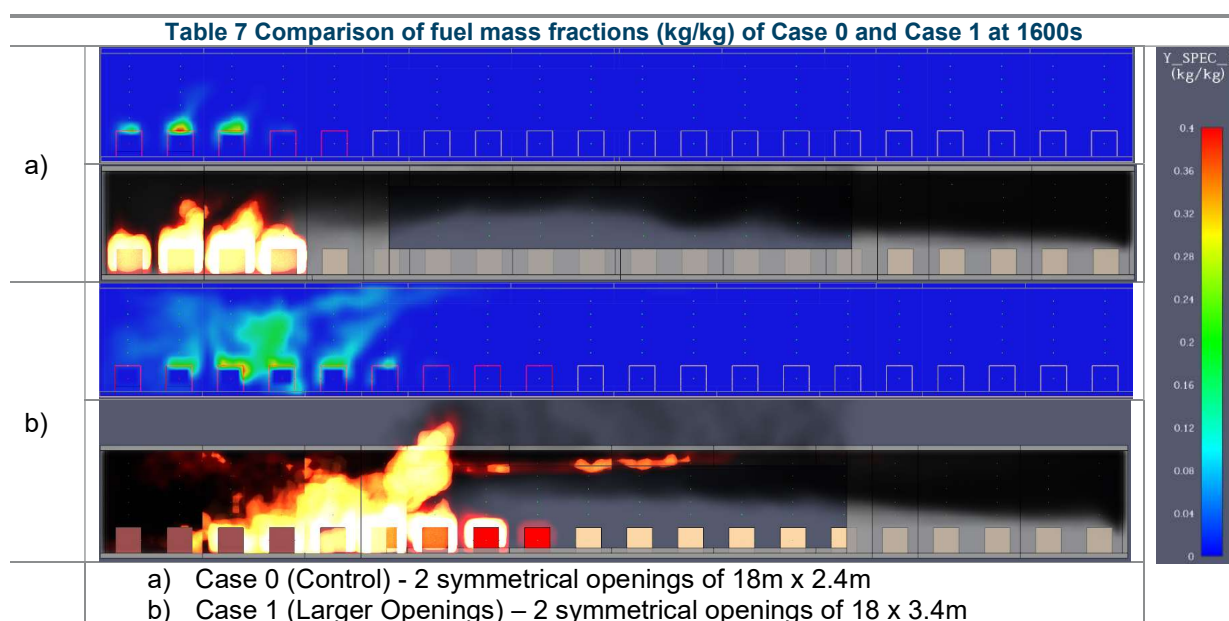


Figure 21 Temperature-Time Profile for different ventilation conditions at (26.9,5.0)

6.1.2.1 Larger Openings

In Case 1 (Larger Openings) the temperatures escalate at a quicker rate and peaks at 1000°C. This is contrasted with Case 0 (Control), where the peak temperature does not exceed 800°C. The increased opening area in Case 1 supplies a larger amount of fresh air to the compartment, allowing more efficient combustion at the early stages of the fire. The larger radiative feedback from the hotter smoke and flames accelerates the fire growth and causes the temperature to rise sharply as seen in Case 1. However, due to a larger amount of fuel packages being involved at this stage, more pyrolysis gases are produced and at a certain point in time, a fuel rich environment is created within the compartment. The flames consequently become extended in height explaining the higher peak temperatures observed in Case 1. The fuel rich environment does not occur as severely in Case 0 because of the initially lower fire spread. Table 7 shows a comparison of the fuel mass fractions, contrasting the fuel rich environment in Case 1 associated to increased flame length and higher ceiling temperatures.



6.1.2.2 Location of Openings (Openings placed at the short ends of the compartment)

Similar to the observations in Section 6.1.1, a second peak in temperature is recorded just prior to burnout of the compartment in all but one case. The characteristic localised flashover at the end of the compartment is absent in Case 3 (Ventilation openings at the short faces) due to the hot smoke being able to readily escape through the openings. Figure 22 confirms that the fire spread in the Case 0 (Control) is initiated by the hot smoke layer whereas fire spread is triggered by the flames of the adjacent fuel packages in Case 3. In all simulations, the trigger event for flame spread was based on the fuel packages' surface temperature. This temperature was set at 300°C and is denoted by the green horizontal line in the graph. In the Case 0, the top face of the fuel package reaches the ignition temperature before the side face, as opposed to Case 3 where the reverse is observed thus supporting the hypothesis that the smoke is not the dominant cause of fire spread in Case 3, unlike in Case 0. These are highlighted by the arrows in Figure 22.

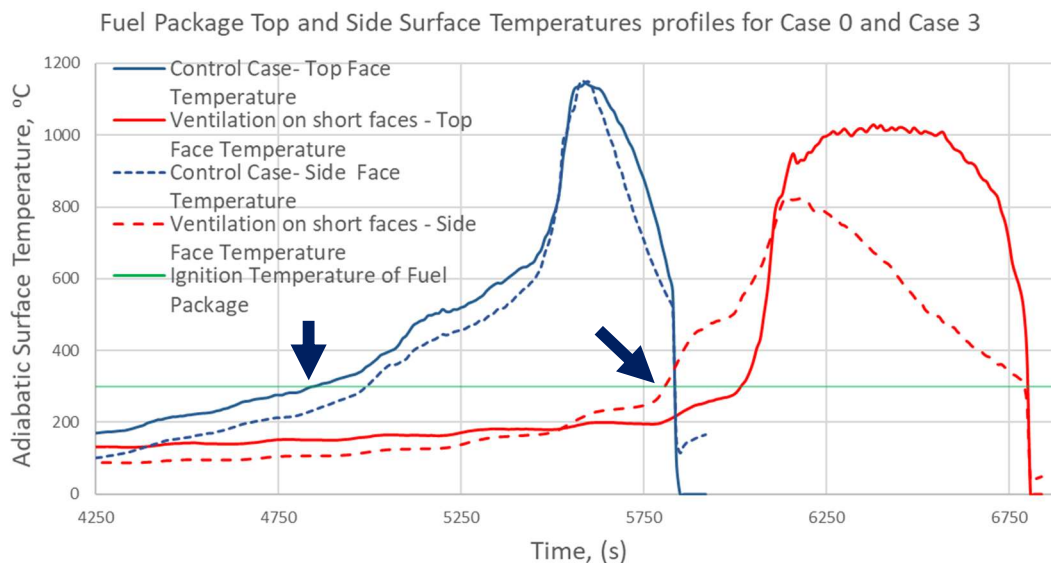


Figure 22 Comparison of Top and Side temperature profiles of fuel package 98 (38.9,5.0) for Case 0 and Case 3

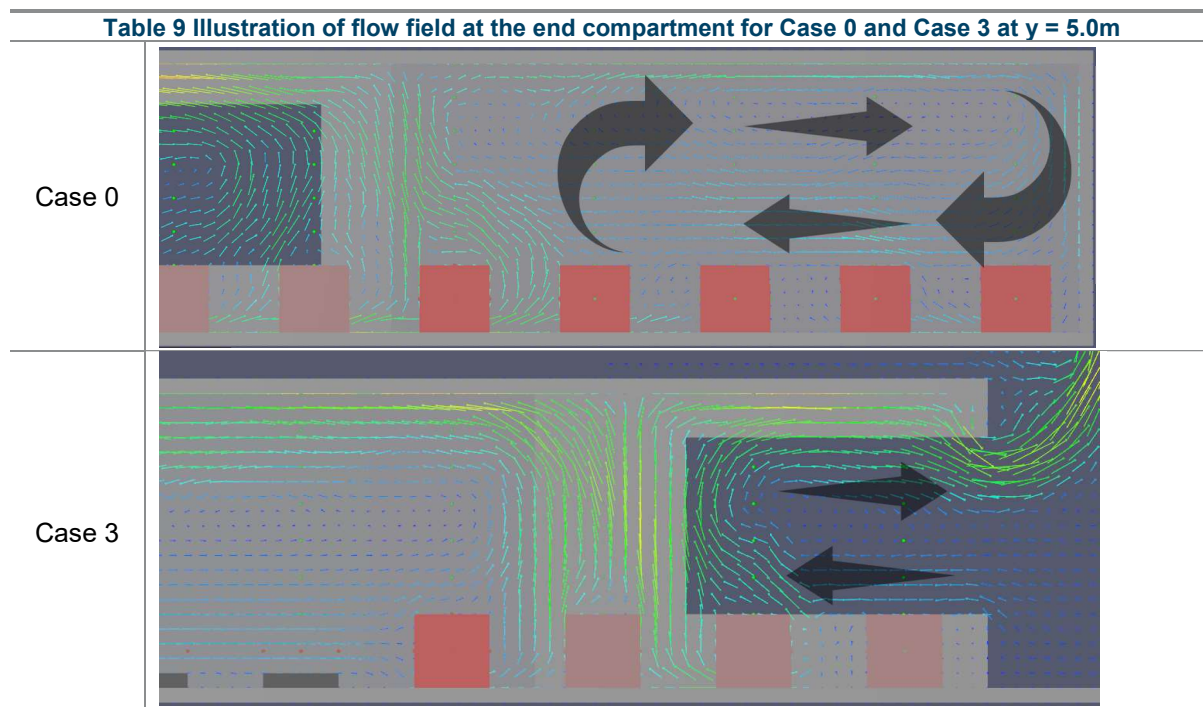
The flow velocities are also presented in order to provide an indication of the flow field prevailing in the compartments. The figures shown correspond to those taken at a height of 3.6m (above the neutral plane and within the smoke layer). A marked difference is that the gas velocities lie mainly between 3.2 to 5.6m/s whereas velocities of 3.2 to 8m/s are observed in the control case. Moreover, the flow velocities recorded in Case 3 are much more homogenous both in magnitude and in space throughout the fire event. This behaviour is heavily contrasted in Case 0 where the velocities peak at 8m/s when the fire front is behind or ahead of the openings.

Table 8 Comparison of velocity flow field of Case 0 and Case 3 at different times at z = 3.6m

Time (s)	Case 0 (Control Case)	Case 3 (Ventilation on short faces)
1600		
3600		
5000		

Velocity scale (m/s): 0, 0.8, 1.6, 2.4, 3.2, 4.0, 4.8, 5.6, 6.4, 7.2, 8.0

The velocity vector slices shown in Table 9 further highlight the trapped smoke recirculation occurring in Case 0 when the flame front progresses past the opening. In Case 3, the lower part of the compartment consists of cold fresh air flowing into the compartment. The cumulative effect of the fresh air ingress and thinner smoke layer lead to the significantly different temperature time profile recorded for Case 3.



6.1.2.3 Decrease in Ventilation Factor

An asymmetrical ventilation condition is induced by removing one of the openings from the control case. Figure 19, Figure 20 & Figure 21 show that higher peak temperatures, of the order of $1100^{\circ}C$ are registered at ceiling level. The fire develops rapidly due to the formation of a thicker smoke layer caused by the presence of only one opening through which the hot gases can escape. Multiple fuel packages being involved in the fire create a fuel rich environment in the compartment, especially with decreased ability to entrain fresh air in. Flaming thus extends to the ceiling and through the openings, explaining the higher peak temperatures. This case exhibits the highest peak temperature in the simulations where ventilation was altered. Interestingly, the peak temperature is recorded when the flame front is at the position $x=20.9m$, despite being adjacent to the opening. This is contrasted with Case 0, where lower temperatures were observed due to increased venting of smoke. These findings indicate that one cannot directly assume lower temperatures will be observed close to openings.

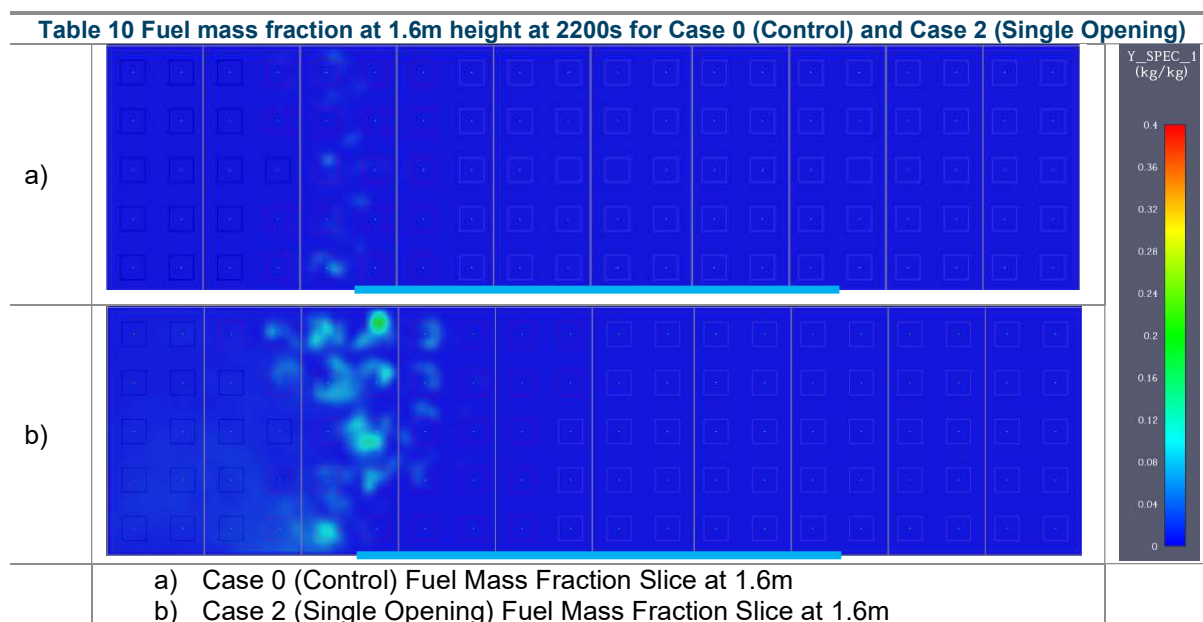
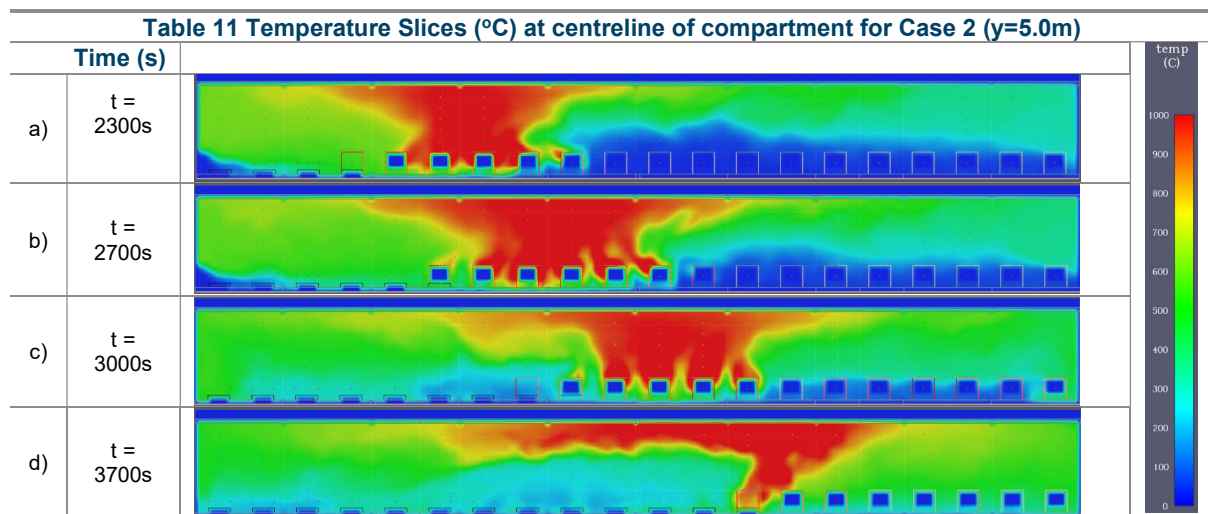
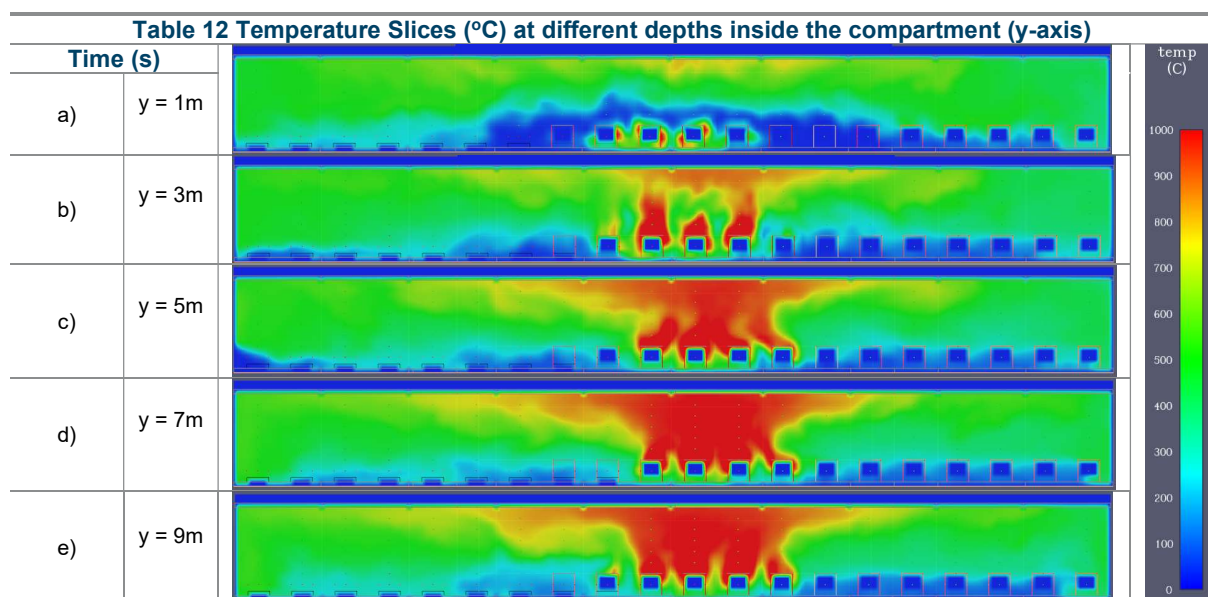


Table 10 compares the fuel mass fraction within the compartment at a height of 1.6m supporting the reasoning that the vitiated oxygen environment causes more significant ceiling jets at the openings. It is interesting to note that the flame jets persist for a larger portion of the fire in this configuration because of limited oxygen availability; the flaming shifts from inside the compartment to the openings, This is reflected by the high ceiling temperature at the 20.9m mark shown in Figure 20.

Furthermore, comparing the temperature slices for the Case 0 (Table 6) and Case 2 (Table 11) reveal that the thermal exposure of 1000°C on the ceiling is much broader in width. The larger area of effect of the elevated temperatures could imply more severe thermal attack of structural elements. Although the scope of this thesis does not include the thermal response analysis of structures, it would be interesting to consider its effects in further research.



The single opening also gives rise to an asymmetrical temperature distribution across the depth of the compartment (y- axis). The temperature slices in Table 12 indicate that the gas temperatures close to the openings are of the order of 700°C (Table 11a)) whereas the temperatures at the back of the compartment (y=9.0m) lie closer to 1000°C. Once again, the impact of the ventilation arrangement cannot be understated; the thermal attack outlined in Figure 23 shows that the back of the compartment is subjected to a more severe temperature for half of the duration of the fire event (shaded in red) which could potentially lead to structural failure induced by uneven heating.



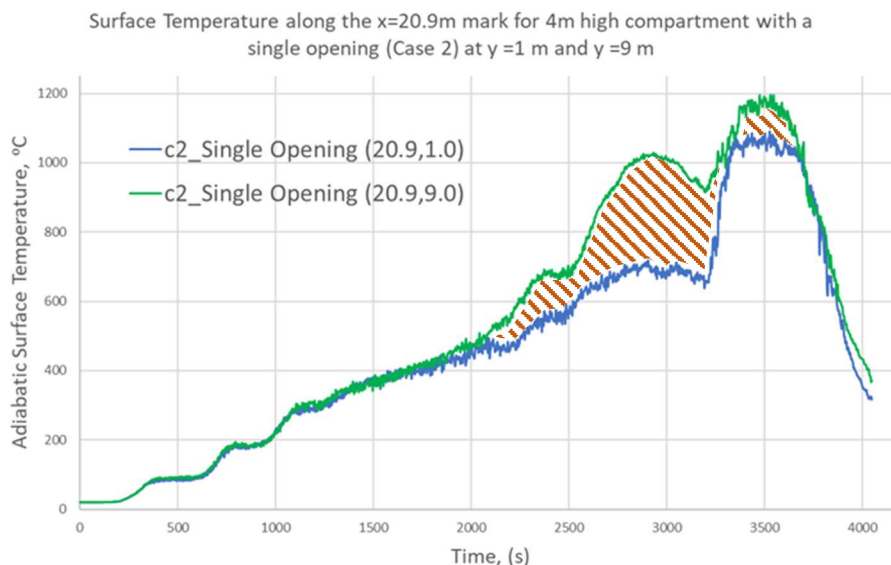


Figure 23 Ceiling Temperature (°C) for single opening case showing difference in thermal exposure

6.1.2.4 Dynamic ventilation conditions

Case 6 (Simulated Window Breakage) shows multiple similarities with the cases discussed earlier. Prior to the window breakage, the exhaust of smoke is limited and causes the smoke layer to descend to about 1.5m as shown in Table 13. The increased radiation feedback enhances the propagation of the flame leading to a larger surface area being involved in the fire. However, the fire is heavily ventilation controlled at this point due to the limited openings. Upon breakage of the window, the ingress of air allows the fire to grow rapidly leading to peak ceiling temperatures of 1000°C. The simulated window breakage scenario provides important insights as to how the initial ventilation conditions can impact on the fire progress and temperature inside a compartment and thermal exposure as demonstrated in Figure 19, Figure 20 & Figure 21.

Table 13 Comparison of smoke layer heights before and after first set of windows break	
a)	
b)	
a)	Smoke layer prior to window breakage (t =1460s)
b)	Smoke layer after first set of windows break (t =1598s)

Based on the results presented, it is evident that the ventilation conditions play a significant role on the temperature profiles inside a compartment. Localised flashovers were observed in compartments where smoke could not readily escape ahead of the flame front causing a secondary high temperature exposure to elements at the ceiling. Additionally, it was inferred from Case 1 and Case 2 that the peak registered temperatures did not behave in a consistent fashion with regards to the supply of fresh air; both increasing and decreasing the opening size led to higher temperatures than the control case. The

peak temperatures recorded varied from 600°C to 1100°C in the five cases studied. Furthermore, Case 6 demonstrated that dynamic changes in the compartment ventilation can lead to large deviations in fire behaviour and should therefore be taken into consideration when studying thermal effects on a structure. The high sensitivity to ventilation demonstrated in the above cases is certainly a contributing factor in the challenge to obtain accurate results from a-priori generated models [48].

6.1.3 Compartment ceiling height and travelling fire behaviour

The following graphs illustrate the effects of compartment ceiling height on the temperature-time profile. Three different ceiling heights namely 3m, 4m and 5m are compared and depicted in Figure 24, Figure 25 and Figure 26. The legend applies to Figure 24, Figure 25 and Figure 26.

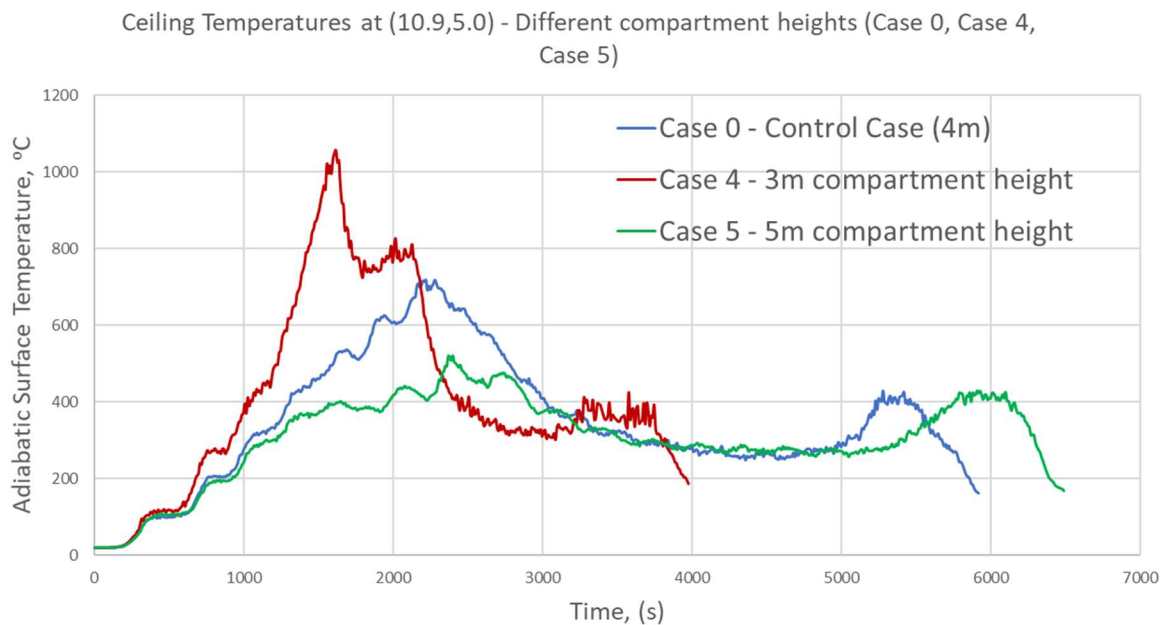


Figure 24 Temperature-Time Profile for different ceiling heights at (10.9,5.0)

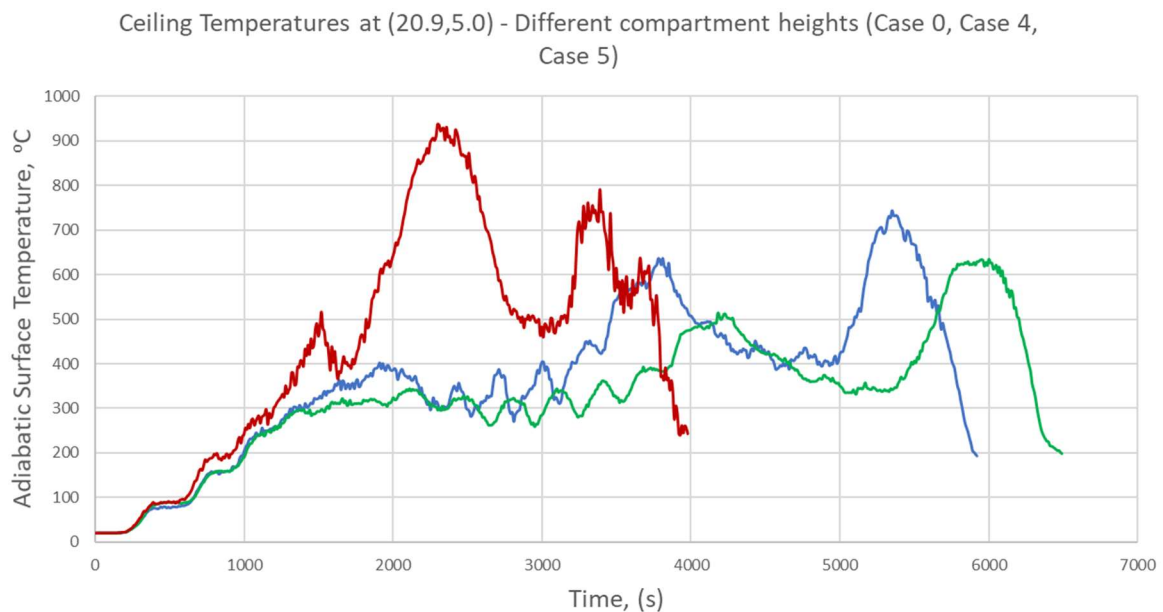


Figure 25 Temperature-Time Profile for different ceiling heights at (20.9,5.0)

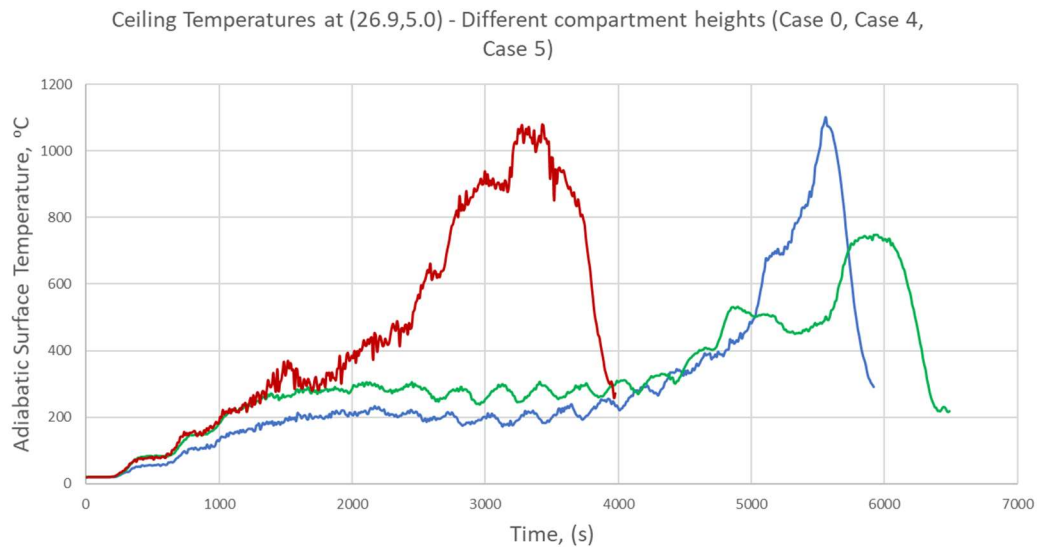


Figure 26 Temperature-Time Profile for different ceiling heights at (26.9,5.0)

The results reveal that lower compartment heights are associated with faster rise and higher peak temperatures and this is attributed to flame impingement on the ceiling (see Table 14). The fire growth is also accelerated by the flame radiation from the ceiling jets to the fuel packages underneath. Figure 27 shows how the incident heat flux on the top face of the fuel package is much more significant the lower the compartment ceiling is. This causes the heat release rate to rise sharply and contribute to temperatures in excess of 1050°C. Due to the rapid fire growth, the fire travels quickly to the end of the compartment; burnout is reached after 4000 s only. In comparison, Case 0 and Case 5 take 5900s and 6450s respectively. In scenario with a 5m compartment height, only transient flame impingement occurs resulting in slower fire spread overall.

Table 14 Side view of 3m and 5m compartment showing extent of flame impingement and ceiling jets	
a)	<p style="text-align: center;">Severe flame impingement: Arrow indicating flame arching over next row.</p>
b)	<p style="text-align: center;">Minimal flame impingement on ceiling</p>
a)	3m compartment height
b)	5m compartment height

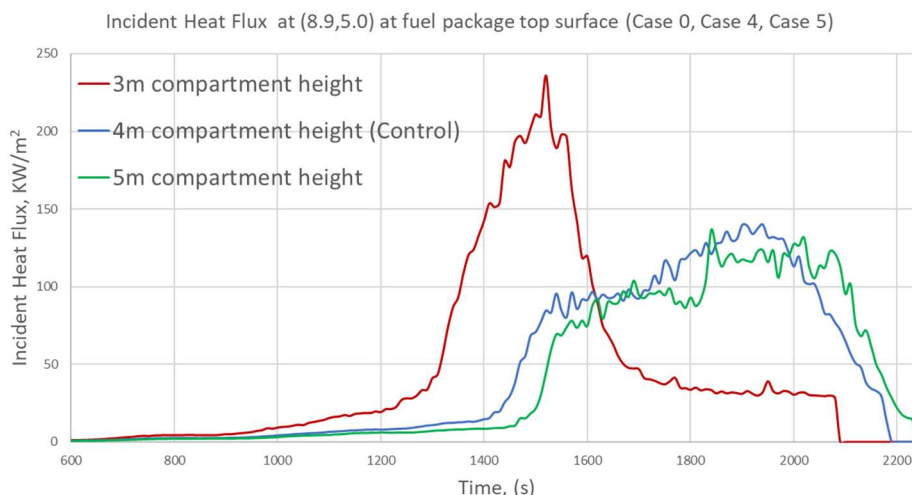


Figure 27 Comparison of Incident Heat Flux of top face of fuel package 18 (8.9,5.0)

6.1.4 HRRPUA and Travelling Fire Behaviour

The influence of an increased HRRPUA (Case 7) is compared to the control cases in the three following graphs. The results show that more severe thermal exposure is encountered in the increased HRR case due to the significant flame impingement occurring at the ceiling; temperatures of the order of 1200°C are registered at all three locations at which the temperature was plotted. Moreover, the far field temperature remains elevated due to the higher energy released during the course of the fire. As a result, the fire progresses through the compartment at a faster rate leading to burnout after only 52 minutes. It should also be noted that significant external flaming is observed in Case 7, explained by the fuel rich environment produced by the higher HRRPUA.

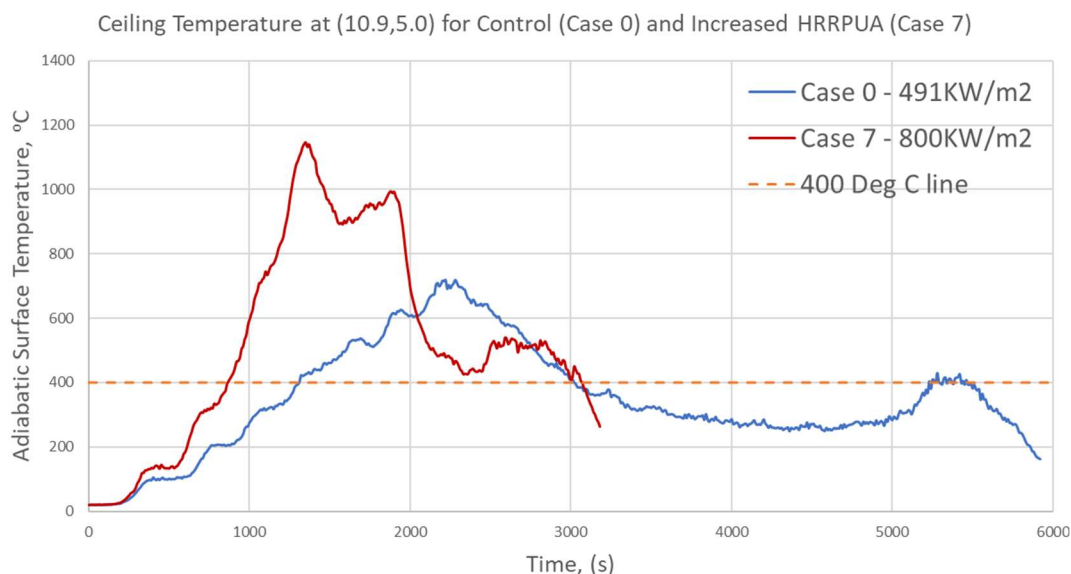


Figure 28 Temperature-Time Profile for different HRRPUA at (10.9,5.0)

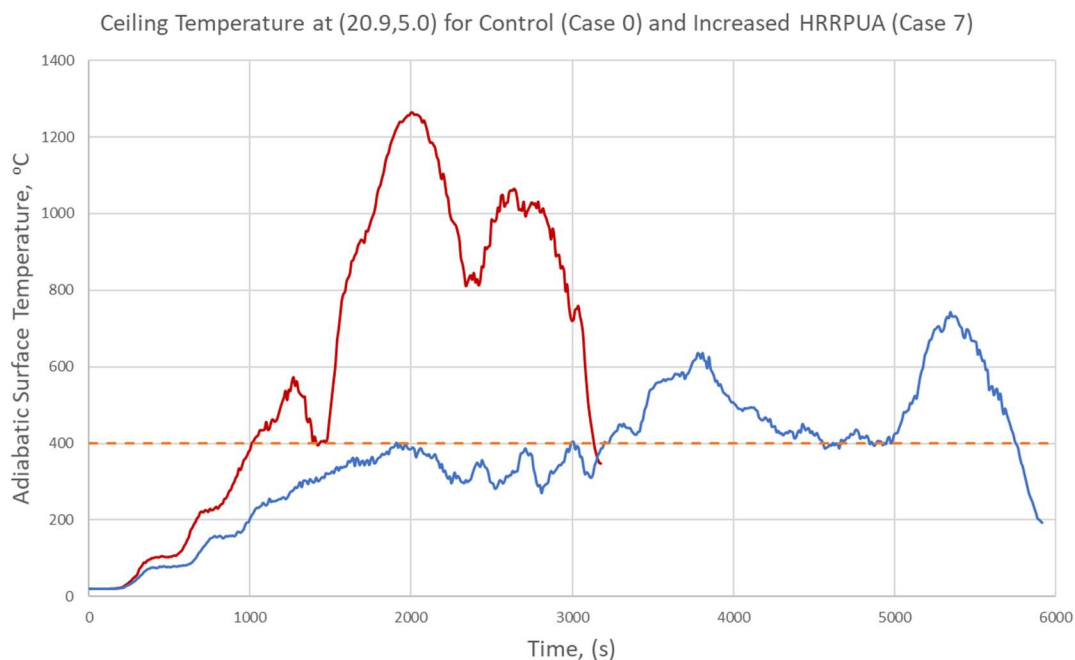


Figure 29 Temperature-Time Profile for different HRRPUA at (20.9,5.0)

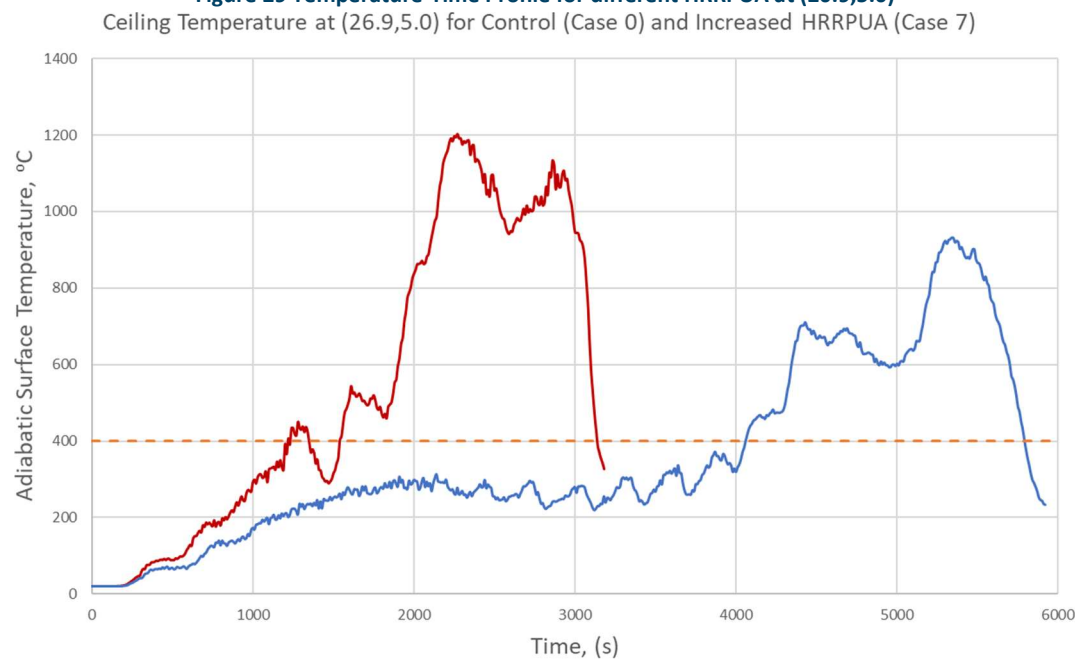


Figure 30 Temperature-Time Profile for different HRRPUA at (26.9,5.0)

It is inferred from the results that an increase in HRRPUA leads to a shorter burn duration but at more severe temperatures. It is however noted that the duration at which the temperatures remain above 400°C are quite similar in both cases as shown in Table 15.

The duration of elevated temperatures beyond 400°C is expected to be of larger importance from a structural design standpoint especially in steel construction due to their rapid strength loss past 400°C. However, despite a 40% increase in HRRPUA, the exposure times remained fairly similar to the control case. These findings imply that the structural response in those cases will be dictated by the magnitude of the temperature, rather than the duration. It is thus proposed that the impact of thermal effects on the structural strength are carried out in future works to quantitatively assess the difference in structural response. Further simulations are also suggested to confirm whether the exposure to >400°C remains relatively constant over a broad range of HRRPUA values.

Table 15 Comparison of key results obtained from Case 0 and Case 7 simulations				
	Units	Control (Case 0)	Increased HRRPUA (Case 7)	
HRRPUA	KW/m ²	491	800	
Time to burnout	minutes	98	52	
Peak Temperature	°C	925	1250	
Time temperature >400°C	minutes	x=10.9m	28	37
		x=20.9m	35	35
		x=36.9m	29	28

6.1.4.1 Compartment Geometry and travelling fire behaviour

In this section, the impact of the compartment geometry is analysed. It should be noted that the plots in Figure 31 are measured at the centreline of the compartment at a distance of 11m from the fire origin. Despite that all parameters such as HRRPUA, number of fuel packages, ventilation sizes have been kept the same, disparate fire behaviours are observed between the two scenarios.

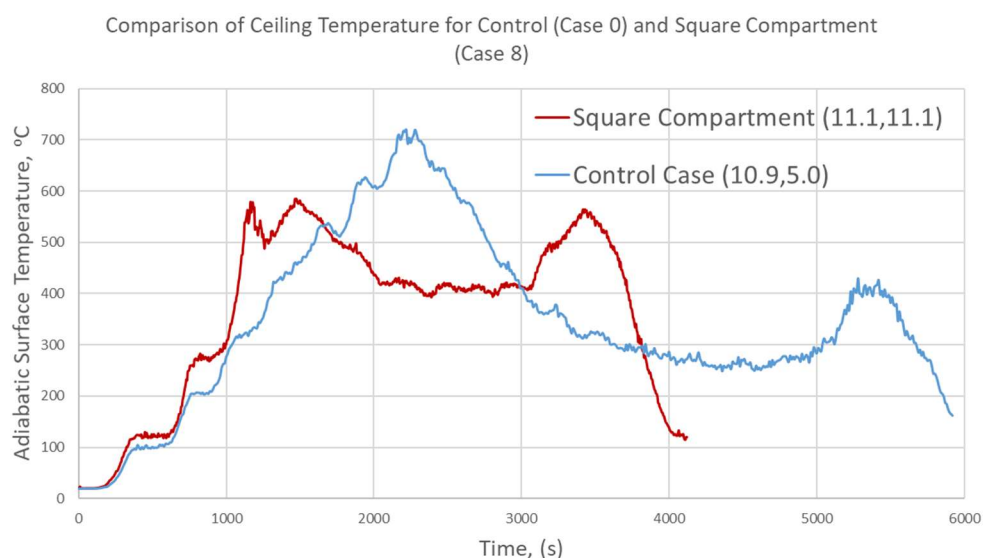


Figure 31 Temperature-time profile (°C) at centreline of compartment (y=5.0m for case 0, y=11.1 for Case 8) showing geometry effects on travelling fire behaviour

The fact that burnout is reached earlier in the square compartment indicates faster fire spread within the compartment. As shown in Figure 32, the fire spreads radially from the ignition source but is subsequently restricted by the compartment walls in the control case causing the flame front to spread to transition from a radial pattern to a linear one. On the other hand, because of the larger width of the compartment in Case 8, the fire spreads freely in a radial manner as illustrated in Figure 33. For this reason, burnout is reached faster in Case 8 than in Case 0.

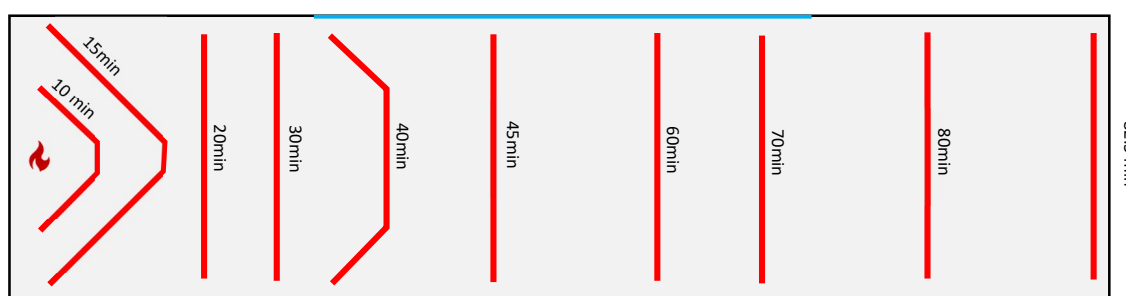


Figure 32 Mapping of Flame front for control case 4m height (Case 0)

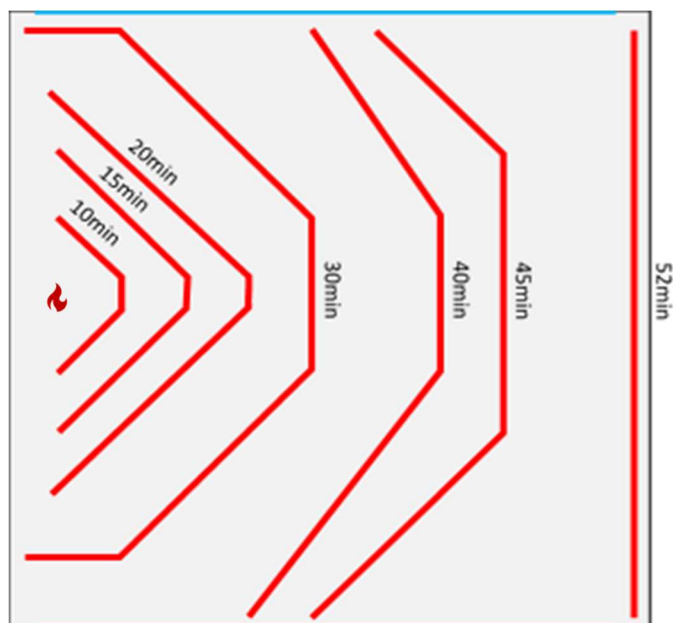
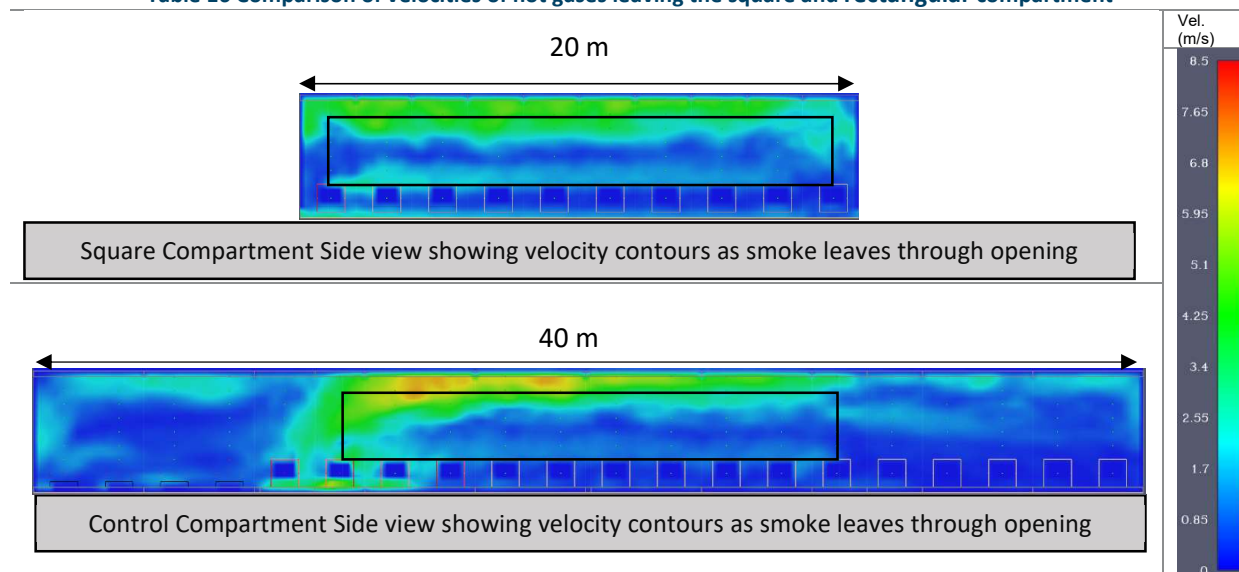


Figure 33 Mapping of Flame front for Square Compartment (Case 8)

The plots also reveal a rather counterintuitive behaviour; the peak temperatures are lower than the control case despite showing a faster and more vigorous fire growth. This behaviour is related to the position of the ventilation openings. In Case 8, less hot smoke and by extension, heat, is trapped in the compartment because the openings occupy the entirety of two of the wall faces. The hypothesis is confirmed when observing the velocity profiles at the openings, shown in Table 16; velocities as high as 8.5m/s are recorded in the rectangular compartment as hot smoke is channelled first by the side walls, then through the openings. The absence of such obstructions in the square compartment gives rise to velocities inferior to 6m/s. It is thus inferred that a higher fire spread rate does not necessarily lead to a more severe thermal exposure of the ceiling. This example thus further stresses the complexity associated of ventilation openings on predicting temperatures inside a compartment.

Table 16 Comparison of velocities of hot gases leaving the square and rectangular compartment



6.2 IMPLEMENTATION OF TRAVELLING FIRE METHODOLOGY

The TFM is applied with the same boundary conditions used in the numerical simulations and making certain assumptions, as mentioned in Section 4.2.2 and 5.2. In this section, we assign a fixed fire spread rate value which is required to plug into the TFM formulae. Although the intent of the calculation-based travelling fire methodology is to obtain temperature profiles without having to resort to numerical simulations, the large band of fire spread rates retrieved from literature impart a large amount of uncertainty to the accuracy of the methodology. Initially, an average value of 10.4mm/s was used as described in Section 5.2.1. Using this method, the results matched very poorly with the simulation results and was thus not applied further in this study. More details about this method can be found in Appendix 10.2. As an alternative method, the average fire spread rate used in the calculations is based on the burnout time of each respective scenario based on FDS simulations using the equation Eq. 20 . The average fire spread rates are found to be in agreement with fire spread rates (between 1.5-19.3mm/s) reported for natural fires in large scale compartments [4]. The approach used also ensured that the burnout of the compartment in the TFM curves corresponded with the results from the simulations. Additionally, a near field temperature is also specified to cap the maximum temperature experienced at any point at the compartment ceiling. This value is set based on the peak temperature observed in the simulations studied in this thesis while remaining within the 800-1200°C bounds set by the methodology.

$$s_{avg} = \frac{L}{t_{burnout}} \quad \text{Eq. 20}$$

Where $L = \text{Length of compartment, (m)}$

$s_{avg} = \text{average fire spread rate, (mm/s)}$

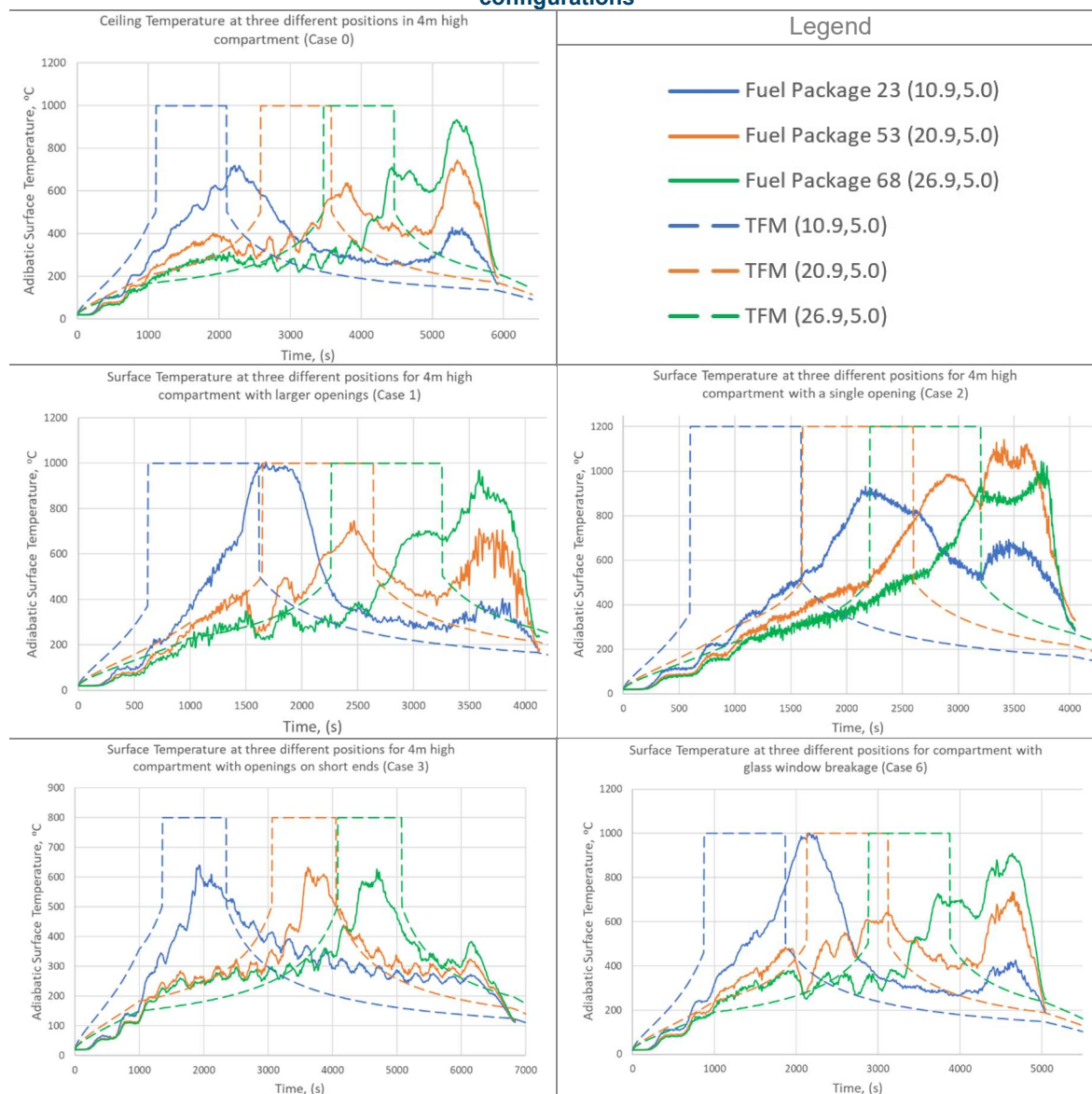
Scenario	Time to burnout, (s)	Average fire spread rate, s_{avg}
Case 0 – Base Scenario	5896.8	6.78
Case 1 – Larger Ventilation Openings	4106.9	9.74
Case 2 – Single Opening	4019.5	9.95
Case 3 - Ventilation on short faces	6810.1	5.87
Case 4 – Lower Compartment height	3957.4	10.1
Case 5 – Higher compartment height	6463.8	6.19
Case 6 - Simulated window breakage	5023.2	7.96
Case 7 – Increased HRRPUA	3156.2	12.7
Case 8 – Square Compartment	4094	4.89
Case 9 – Square compartment – different ignition location	4312.8	4.64

Using the above values, the temperature time profiles are plotted and compared. In all the simulations, the adiabatic surface temperature is used to determine the prevailing ceiling temperature. The adiabatic surface temperature is deemed most appropriate because it provides a representation of the fire insult to a structure and can be used directly to evaluate heat transfer to a given specimen as well as its temperature. Studies have also shown that plate thermometers as specified in the ISO 834 and EN 13663-1 standards approximately measure adiabatic surface temperature [49].

6.2.1 Ventilation Configurations and TFM

The TFM does not incorporate ventilation in its calculation procedure explicitly despite Section 6.1 clearly showing a strong influence of ventilation conditions on the shape of the temperature-time curves. The impact of ventilation on the fire behaviour is therefore not predicted by this methodology unless accounted for by other parameters, namely fire spread rate, HRRPUA and fuel load density. In the following graphs, an attempt is made to adjust for the ventilation by using the average fire spread rates summarised in Table 17. The decision is supported by the inability to assume a fire spread rate with low uncertainty. The time temperature profile for different ventilation conditions and locations are presented in Table 18.

Table 18 Comparison of TFM and measured temperature time profiles for different ventilation configurations



The plots show that the TFM temperature-time envelopes are out of phase with the actual recorded temperatures inside the compartment except for Case 3 (ventilation openings on short faces). The offset is most prominent in case 2 (Single Opening), corresponding to the most severe localised flashover case and presenting the highest peak temperatures. Both of these observations hint towards the fact that the localised flashover event could be associated with this offset when superposing the curves. The absence of a localised flashover at the end of the compartment in Case 3 also supports

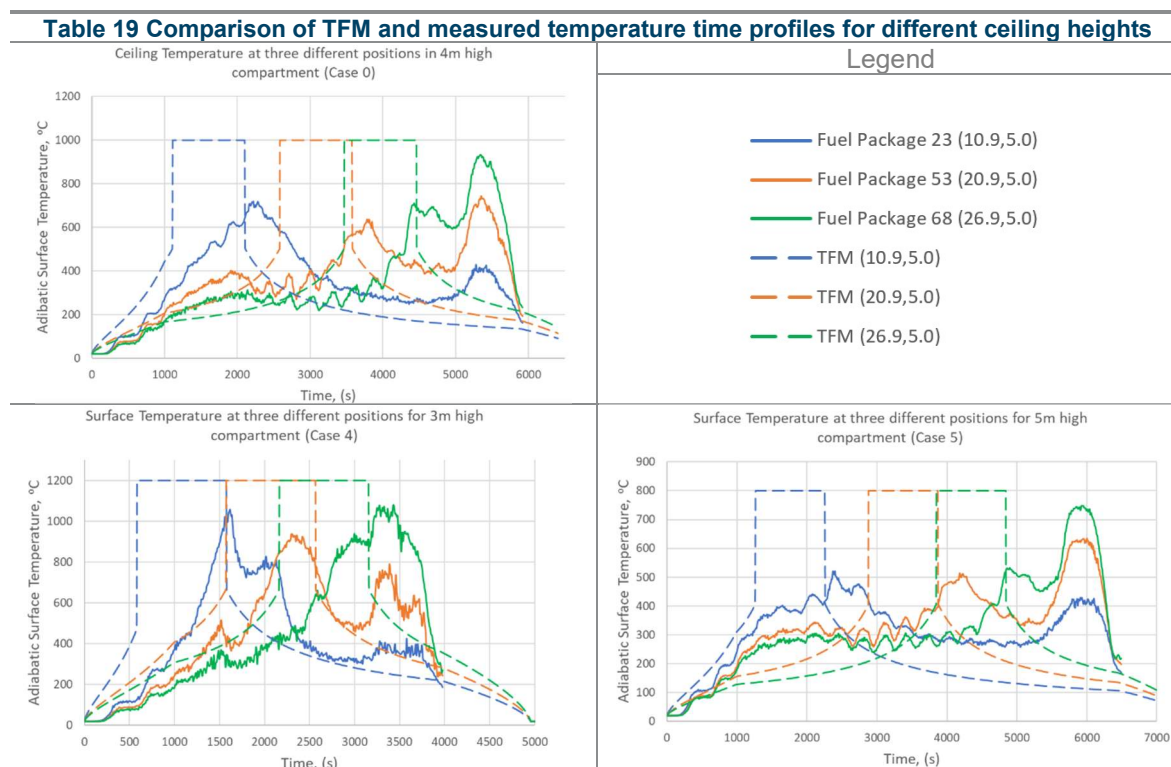
this hypothesis; the TFM curves predict the temperature variation over time quite conservatively for a significant portion of the time under thermal exposure. This hypothesis is further discussed in Section 6.3.

Furthermore, it should be noted that the maximum near-field temperatures set are informed by the maximum recorded temperatures in the simulations. For this reason, the near field temperature is not underpredicted in any of the cases. Nevertheless, in the absence of numerical or experimental information specific to each particular scenario, it is difficult to accurately predict the near field temperature. The upper limit of 1200°C reported in literature can still be used to ensure conservativeness in that respect.

With regards to the far field temperatures, the TFM generates conservative values when the fire is travelling towards the measurement point but underpredicts the temperatures once the fire travels past the point of interest. As observed in several simulations, ceiling jets caused by the end of compartment flashover tend to extend towards the openings, causing high temperatures to be registered prior to burnout of all the fuel. This phenomenon is not captured by the TFM and thus explains the underpredicted far field temperatures. Underpredictions of up to 870°C are noted in Case 2 close to burnout. Additionally, not accounting for the elevated temperatures prior to burnout induce severe inaccuracies in a subsequent thermal response analysis on the ceiling elements. The fact that 4 out of 5 cases studied demonstrate this behaviour warrant the need for further refinement of the TFM prior to application in structural fire safety design. The importance is further compounded upon observation that in Cases 0, 2 and 6, the second temperature peak is of larger magnitude than the first at some locations by 50-100°C. It is also stressed that the TFM assumes a homogenous temperature along the y-axis; this is however, untrue, as highlighted previously in Figure 23.

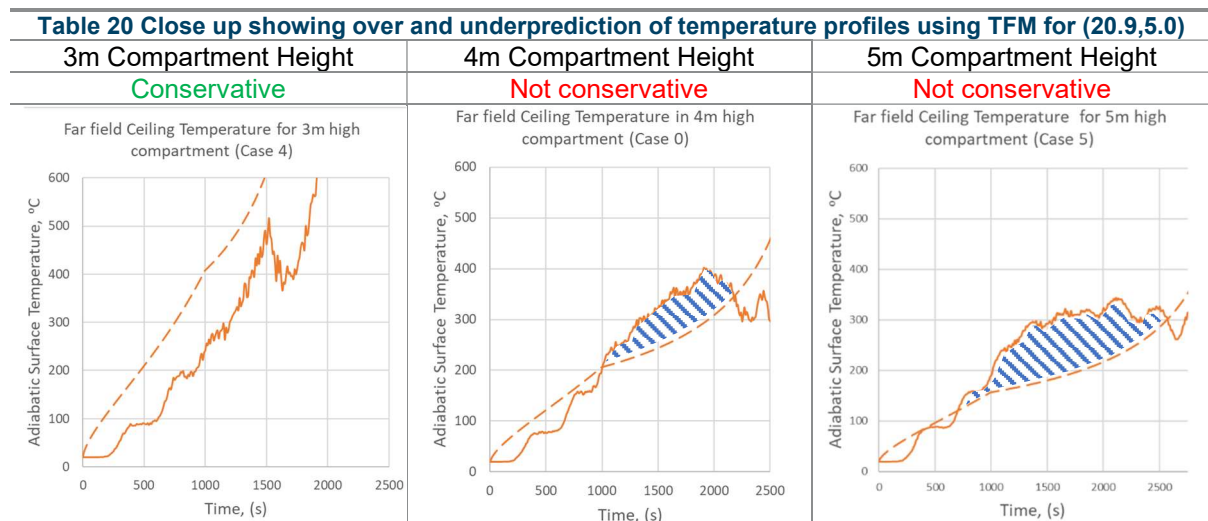
6.2.2 Compartment Height and TFM

In the following set of graphs, the TFM curves are compared to the results for simulations modelling different ceiling heights.



Once again, an offset of temperature predictions is observed. One of the key observations is that the TFM assumes a minimum near-field temperature of 800°C, originating from the reasoning that the near field temperature would be largely attributed to flame temperature. However, In Case 5, where the ceiling is set at 5m, very limited flame impingement occurs in the initial stages of the fire. As a result, the heating effect of the flame itself is diminished and the lower limit of 800°C imposed by the TFM loses its validity.

Furthermore, the results indicate that the methodology produces better predictions for lower ceiling heights; ignoring the flashover event at the end of the compartment, the far-field temperatures produced by the methodology align the most with the simulation results for the 3m compartment. The quality of the TFM results decrease as the height is increased and is confirmed by the increasingly larger area above the prediction line as the height is increased (e.g. shown in Table 20).



6.2.3 Increased HRRPUA and TFM

In the following graphs, the impact of a larger fuel load density is compared to the TFM generated curves. In order to do so, the HRRPUA in the formula is adjusted to reflect the increase modelled in the simulation.

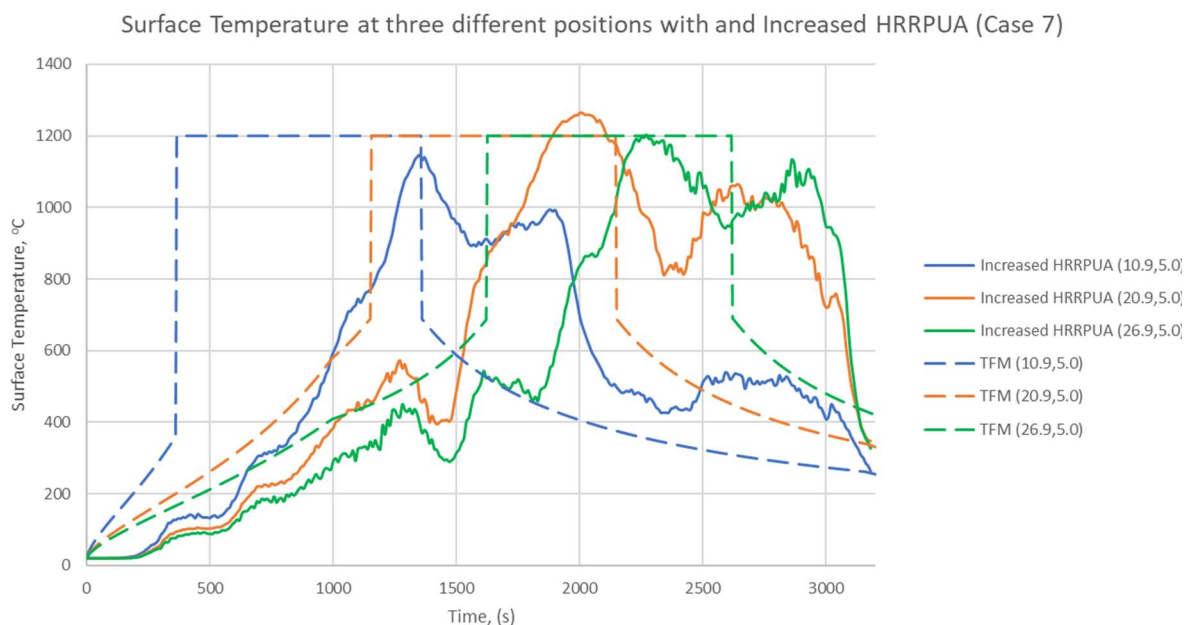


Figure 34 Comparison of TFM and measured temperature time profiles for an increased HRRPUA

The increased HRRPUA is captured by the TFM and predicts the faster rise in temperature observed in the simulations. However, the offset observed in previous cases persists in this scenario as well. Due to the rapid fire progress, the temperature profile remains elevated for a larger portion of the fire event but is not replicated in the TFM results. The discrepancy is most apparent at the measuring point at the centre of the compartment where the openings are located. As explained earlier, this is due to the formation of large ceiling jets moving closer to the openings. The results suggest that the conservativeness of the TFM equations decrease at higher HRRPUA value because of the inability of the TFM to incorporate the heating effects of ceiling jets. The results highlight that the TFM should be applied cautiously, especially when the scenario can give rise to ceiling jets. These can occur not only when the HRRPUA is high but also in low ceiling compartments.

6.2.4 Compartment Geometry and TFM

The comparison of the TFM and the numerical results is also carried out for a square compartment (Case 8). Figure 35 identifies the locations of the probes used in the analysis.

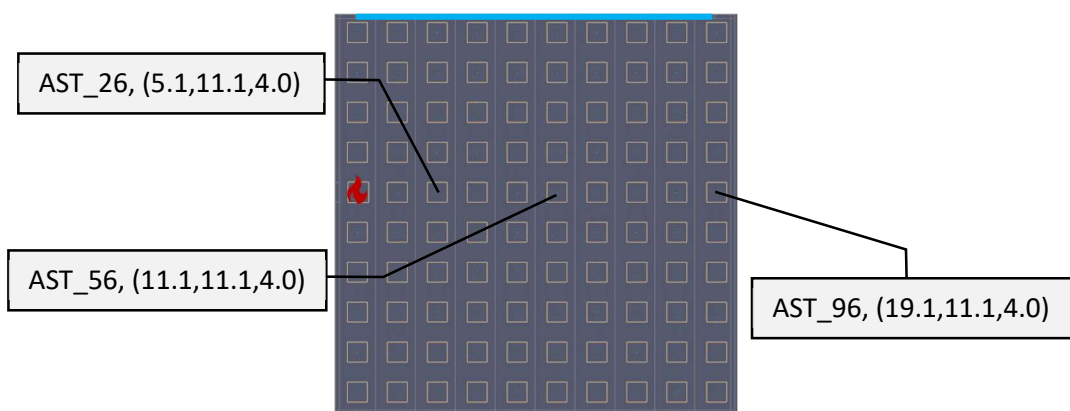


Figure 35 Location of devices measuring temperature profiles in simulations for square compartment

It can be observed that the TFM predicts much more conservatively the temperature profile evolution for the majority of the fire event. Once again, the flashover prior to burn out is not predicted by the methodology causing an underprediction of 250°C in the later stages of the fire at (5.1,11.1) at t=3400s. As illustrated in Section 6.1.4.1, the smoke flows freely out of the compartment in Case 8, like Case 3. The fact that Alpert’s correlation was derived from experiments whereby the smoke was allowed to freely escape from under the ceiling [18] and that the TFM produces better results in cases that replicate such conditions is thus logical. Therefore, it can be inferred that TFM generates better predictions in very well-ventilated cases, where smoke accumulation at ceiling level is minimal.

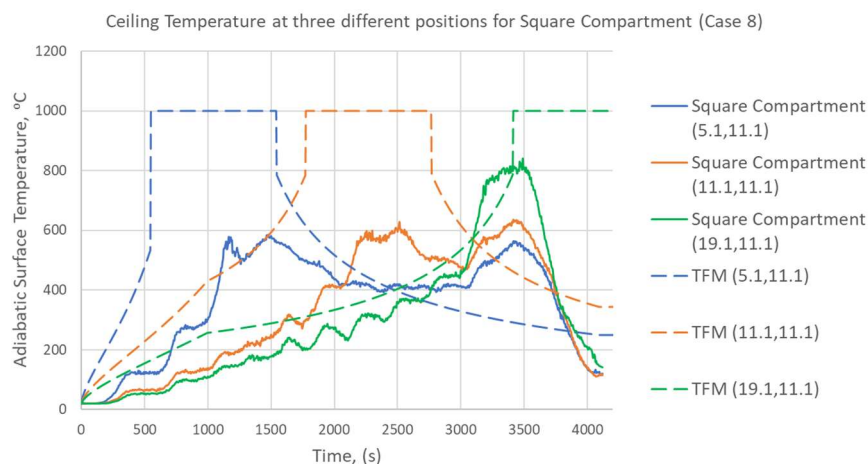


Figure 36 Temperature-Time profile of ceiling at three different positions for Square Compartment (Case 8)

6.3 TFM + HASEMI MODEL FOR FLAME EXTENSION

It was concluded from the previous results that the TFM did not account for the presence of ceiling jets, which in turn led to underpredictions in the temperature field at a given location. In order to address the present oversimplification, Heidari *et al.* [50] developed a method using a combination of the TFM and Hasemi model to estimate the net heat flux resulting from flame extension at the ceiling and hot gases.

In this section, the TFM+Hasemi Model is adapted to reflect the increased heating caused by ceiling jets. It is noted that the Hasemi model was derived from experiments (up to 60MW [50]) with HRR of similar magnitude to those observed in the simulations presented. Since the quality of the mesh does not produce reasonably accurate heat flux values, a comparison of the predicted net heat flux and numerical simulation results is not conducted in this thesis but is proposed for further studies on finer meshes. The implementation of the Hasemi Model is thus limited to making one modification to the existing model. The near field region, which was originally defined as the area lying directly under the fire seat (denoted by L_f in Figure 37), is now increased to cover the regions where ceiling jets are expected to be present (denoted by L_H). The flame extension under the ceiling is calculated using the following equation. The results are presented below for the several cases.

$$L_H = 2.9H \cdot (Q^*)^{0.33} - H \tag{Eq. 21 [50]}$$

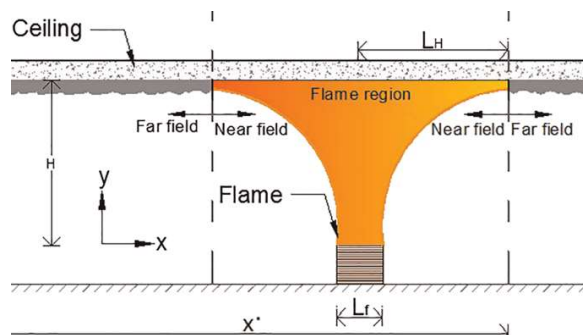


Figure 37 Diagram showing Flame Extension under the ceiling [50]
Comparison of TFM and TFM +Hasemi Model predictions with numerical simulation results (Case 4)

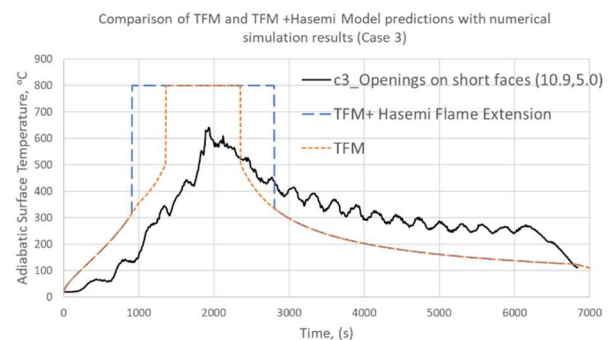


Figure 38 Comparison of TFM & TFM +Hasemi Results for Case 3
Comparison of TFM and TFM +Hasemi Model predictions with numerical simulation results (Case 0)

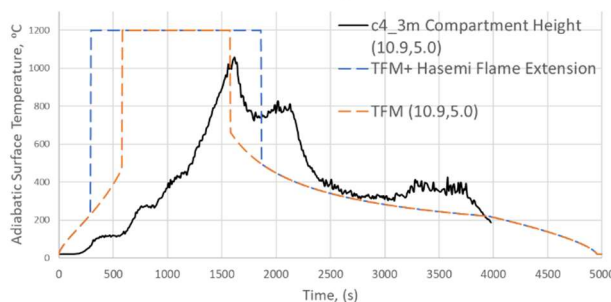


Figure 39 Comparison of TFM & TFM +Hasemi Results for Case 4

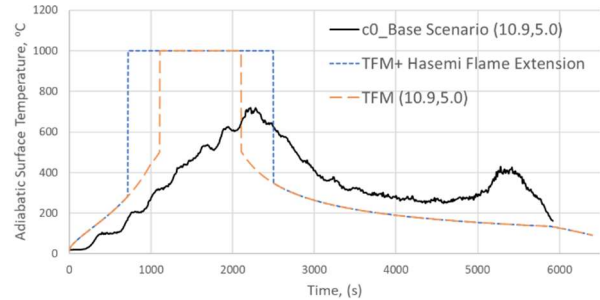


Figure 40 Comparison of TFM & TFM +Hasemi Results for Case 0

The implementation of the TFM + Hasemi method produced mixed results. The revised larger near-field leads to more conservative results. The predictions however do not align with the numerical results obtained. This occurs because the TFM + Hasemi method only changes the near-field temperature profile but not the far-field temperatures. In the above cases, the underprediction of the far-field temperatures as well as the plot offset is still present. Another explanation to the minimal improvement of results is the fact that flame extensions observed in the simulations are not axi-symmetric as assumed by the Hasemi ceiling jet equation. It is also stressed that, despite being simple in geometry, the compartments modelled in this thesis still lead to non axi-symmetric ceiling jets. It is thus concluded that using the Hasemi model to predict the effects of flame extension in travelling fire

scenarios is unreliable due to the complex interaction of the ceiling jets with compartment ventilation and geometry.

6.4 FIRE SPREAD RATES

To implement the TFM, it was required to choose a fixed fire spread rate in the calculation. In this section, the appropriateness of a fixed flame spread is investigated and challenged. The following figures demonstrate the position of the flame front at different time stamps and are used to identify the pattern in which the fire spreads throughout the compartment.

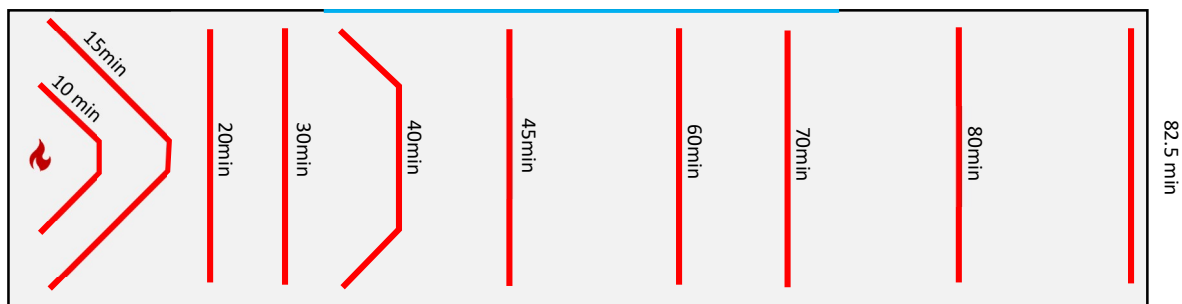


Figure 41 Mapping of Flame front for control case 4m height (Case 0)

It is apparent from Figure 41 that the flame spread occurs in a radial fashion until it reaches the side walls of the compartment, after which the flame spread transitions into a linear flame front. The flame spread accelerates close to the side walls during this transition leading to a non-uniform fire spread rate. More interestingly, the regions close the openings are observed to exhibit slower flame spread. Both these observations emphasize that the presence of obstacles and openings both affect the rate at which the flame front progresses. Already, it can be deduced that the fire spread rate is not constant over the course of the fire. Furthermore, the diagram also shows how the flame spreads at a higher rate at the end of the compartment stressing the gross approximation made when using a uniform fire spread rate in calculations.

The increase in fire spread rate is most apparent in Case 1, as seen in Figure 42, where the over $\frac{1}{4}$ of the compartment is burned through within 10 minutes (20min to 30min mark). It can also be observed that the flame front lingers for 5 mins at 30 metres into the compartment. These indicate that the fire progresses rapidly for the first 40minutes, slows down when past the openings and ending by a flashover at the end of the compartment.

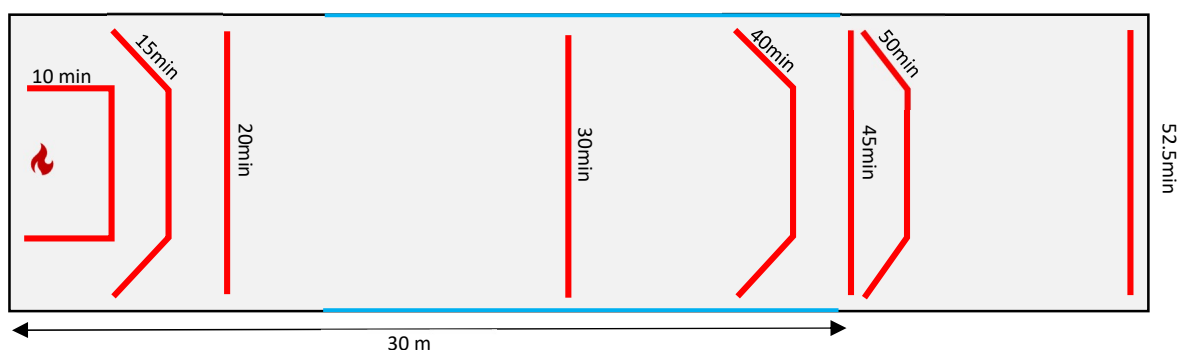


Figure 42 Mapping of flame front positions for increased ventilation case (Case 1)

Figure 43 shows that the presence of an opening leads to the slowing down of fire spread in its proximity. It can be observed that the flame progresses faster on the closed side.

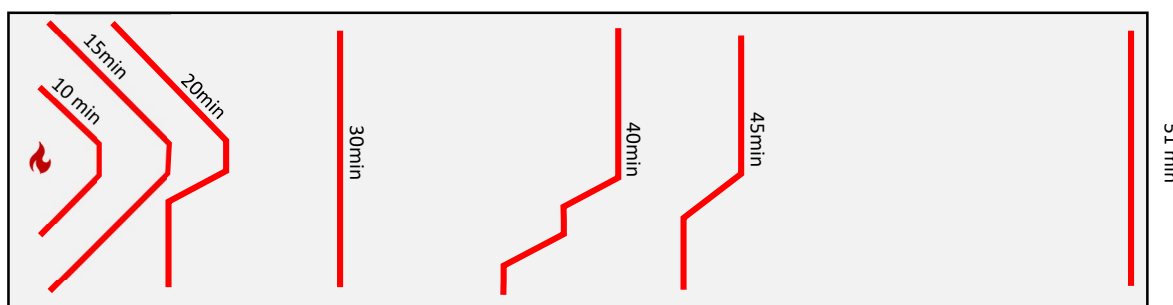


Figure 43 Mapping of Flame Front for Single Sided Opening (Case 2)

Unlike other fire spread patterns seen so far, Figure 44 shows the typical radial flame front transitioning into a linear one. The main difference, however, is that the fire spread rate is uniform over the whole duration of the fire. This can be deduced from the equal spacing of the lines at 10-minute intervals. For this reason, the predictions of the TFM were reasonable in Case 3.

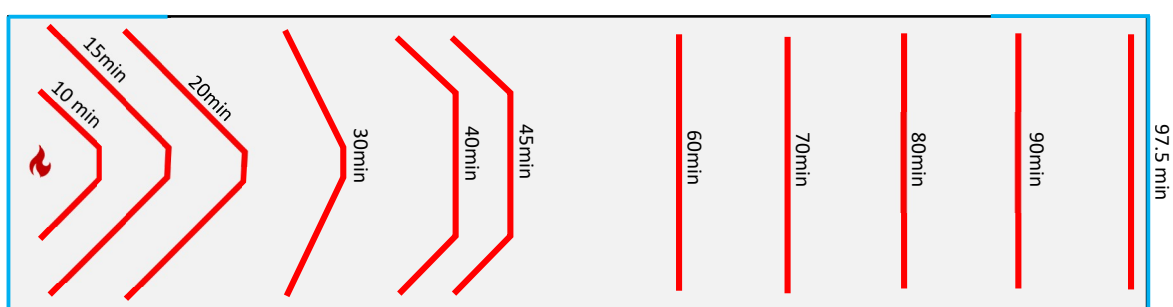


Figure 44 Mapping of Flame Front of short end ventilation openings (Case 3)

Both Figure 45 and Figure 46 show a similar trend to that discussed for Case 0. The fire spread is fastest in the lower compartment height case and the time to burnout increases as the height of the compartment is raised.

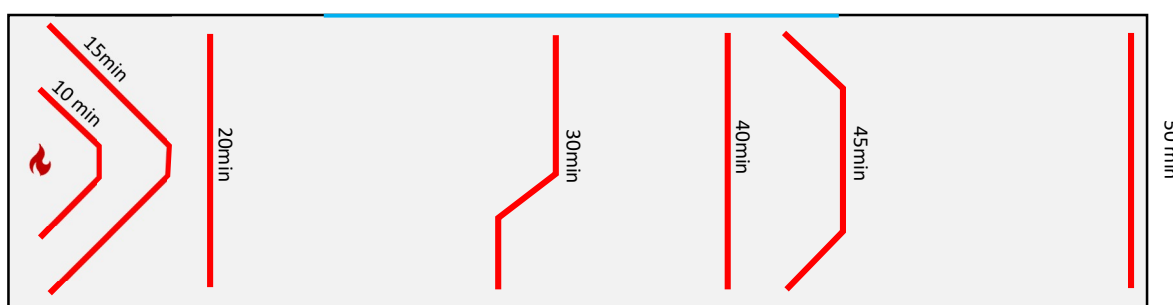


Figure 45 Mapping of Flame front position for 3m ceiling height case (Case 4)

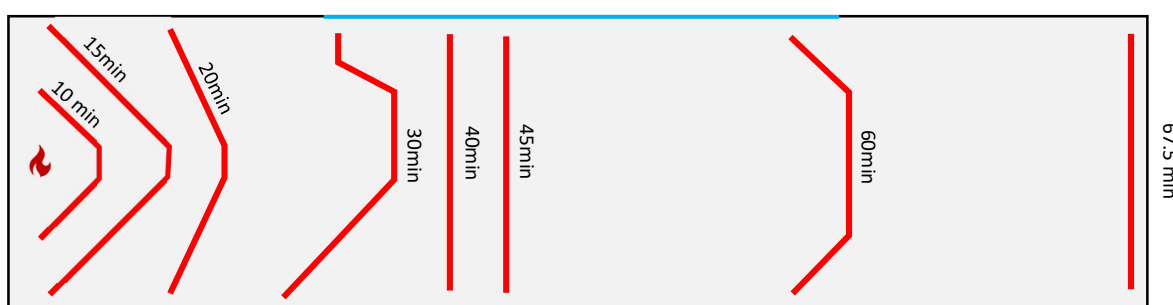


Figure 46 Mapping of Flame Front in 5m Ceiling compartment (Case 5)

Increasing the HRRPUA causes the fire to spread more rapidly than any of the other cases studied. In general, the same flame propagation pattern is seen as in the control case but only at almost twice the rate for a 40% increase in HRRPUA; the average flame spread rate of Case 0 and Case 7 was 6.8m/s and 12.7m/s respectively.

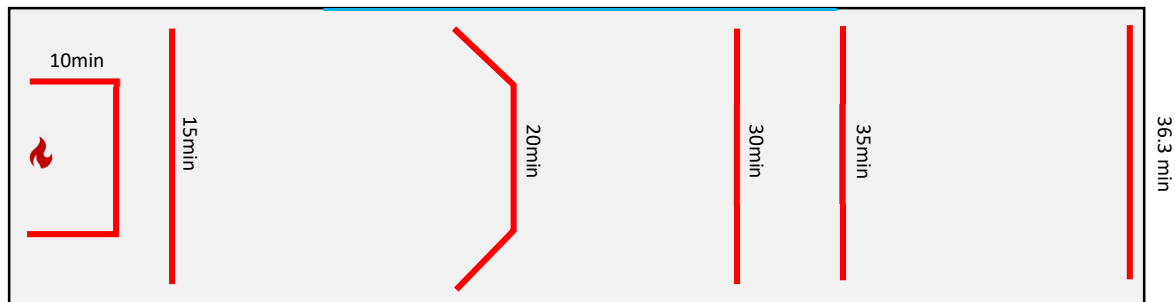


Figure 47 Mapping of Flame Front with Increased HRR (Case 7)

The simulated window breakage scenario (Case 6) indicates that the fire progresses further during the first 30mins of the fire event than the control case because of the initially closed windows. For comparison, the average spread rates calculated for every 10-minute slice is tabulated below.

Table 21 Comparison of Fire Spread rates at 10 min intervals for Case 0 and Case 6		
Timeframe during fire event	Average Flame spread rate (mm/s)	
	Control (Case 0)	Simulated Window Breakage (Case 6)
0-10 min	3.33	3.33
10-20 min	6.67	6.67
20-30 min	3.33	13.33
30-40 min	10.00	6.67

The simple addition of breakable windows to the scenario led to a fire spread rate four times larger than that in the control case for the same time frame (20 to 30mins). It should be noted that the window breakage occurs within this timeframe (t = 25mins). The non-uniform of the fire spread rate is also confirmed from Table 21.

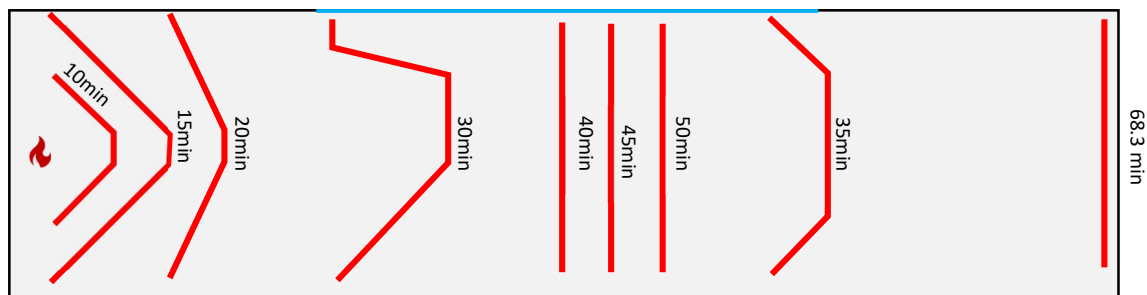


Figure 48 Mapping of flame fronts with simulated window breakage (Case 6)

The 5-minute averaged fire spread rates are plotted for other cases in Figure 49 to gain an insight about the fluctuating flame spread rates in each scenario modelled. The values are obtained by measuring the distance the fire front has advanced after a given time step from the simulations. The fire spread rate is then calculated as follows:

$$\frac{\text{Distance (mm) moved by fire front from time } t_1 \text{ to } t_2}{(t_2 - t_1)} = \text{fire spread rate}_{t_1 \rightarrow t_2} \quad \text{Eq. 22}$$

The plots confirm the fire spread is non constant over the course of the fire event implying that the fixed fire spread rate assumption used in the TFM should be applied cautiously. As observed in the previous chapters, Case 3, which also exhibits a stable fire spread rate, was the scenario that was predicted best using the TFM. The sharp rise in fire spread rate at the end of the burnout is a result of the flashover event explained previously and is thus very large in magnitude. Ignoring this end of compartment phenomenon, we still notice transient peaks of up to 40mm/s in fire spread rate within the first 30 minutes of the fire event. These values greatly exceed the upper limit reported in literature; nevertheless, they did not persist for more than 10 minutes in any of the simulations.

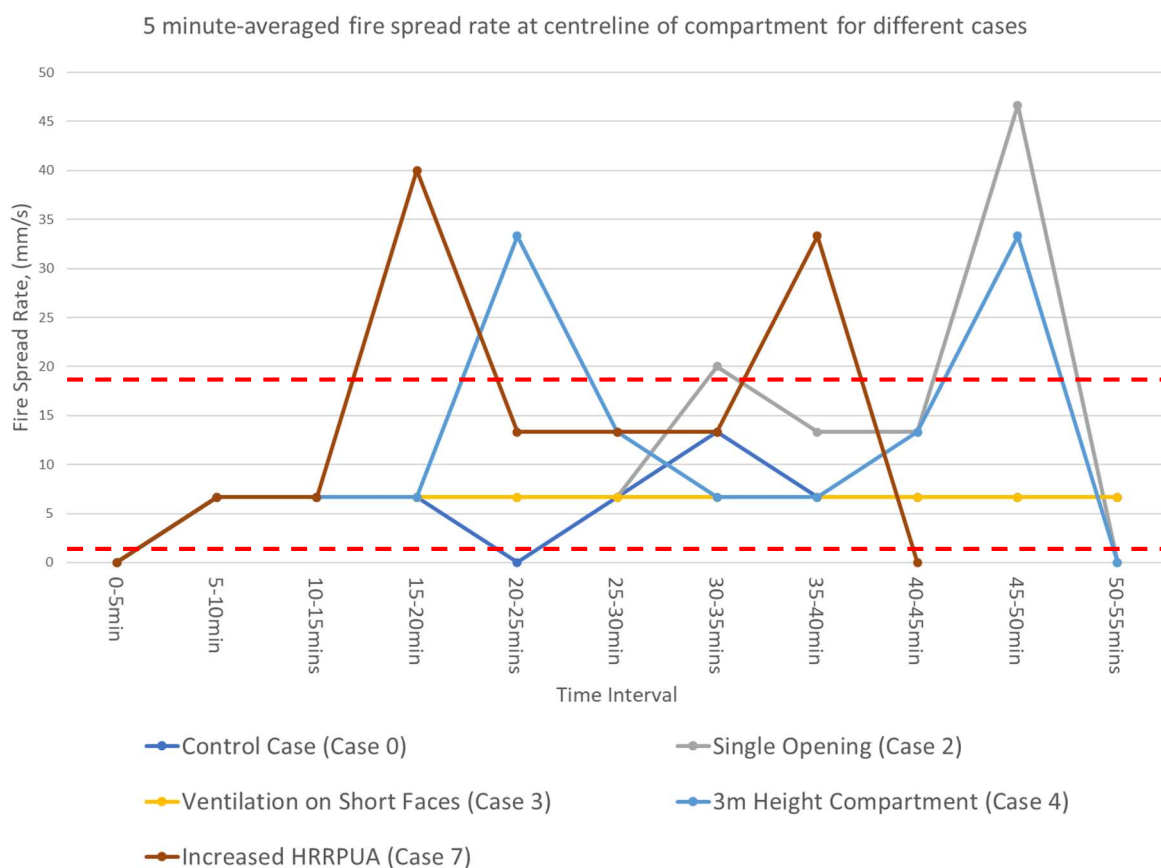


Figure 49 5-minute averaged Fire Spread Rates at the compartment centreline for different cases simulated

It is acknowledged that this procedure could have been refined to a smaller interval, say 1-minute. However, because the fire spread rate is determined based on the discrete locations of the fuel packages, a smaller time interval would lead to erratic values. Already, we notice that the flame spread is nil at the 20 - 25minute mark; this is not the case in reality and is a result of discretized fuel package and small time interval. On the other hand, if too large time intervals are used, say 10-minute, we run the risk of smoothing out fluctuations in flame spread that are inferior to 10minutes in duration. The 10-minute averaged fire spread rate is shown in Figure 50 and highlight how some information is lost and the curve flattened; the peaks are not as large due to the 10 minute averaging procedure.

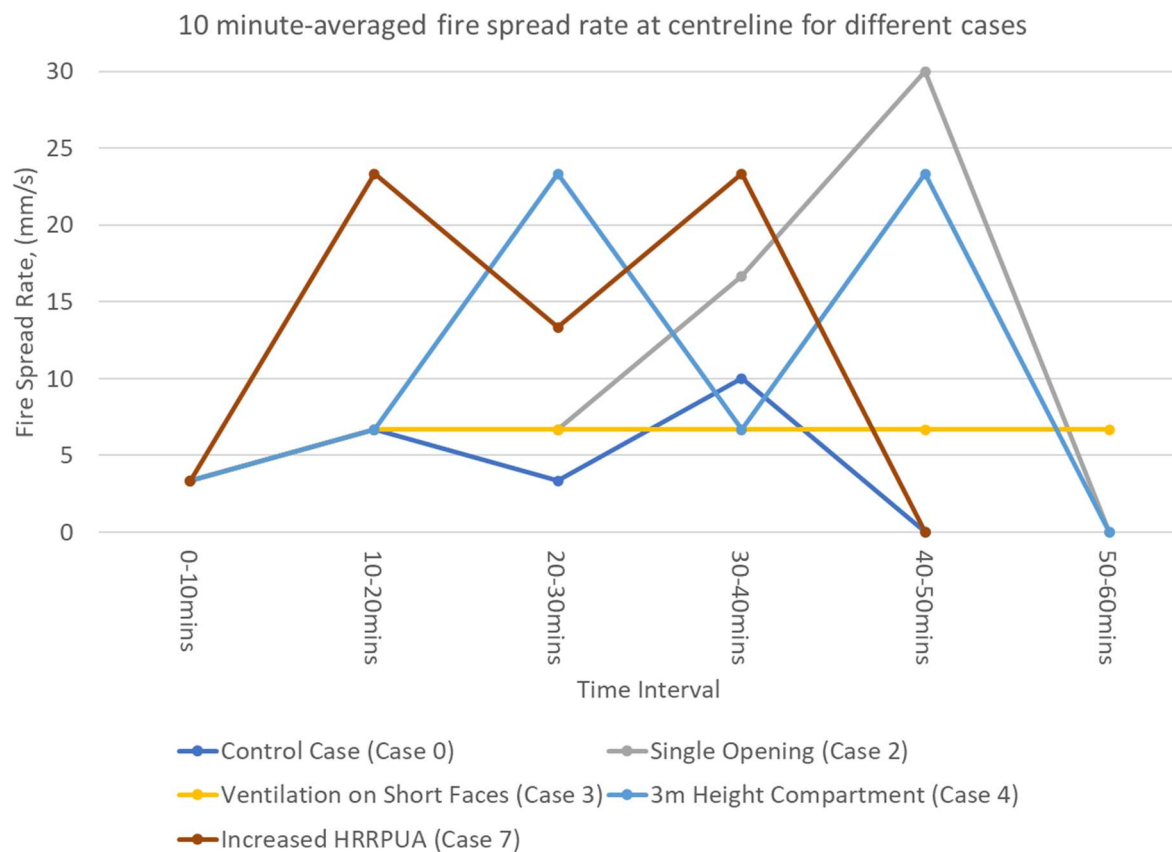


Figure 50 5-minute averaged Fire Spread Rates at the compartment centreline for different cases simulated

From the results, it is concluded that the main limitation in obtaining accurate fire spread rates from the simulations is the discretization of the fuel package. In this particular study, the centre to centre distance between fuel packages was of 2 metres; In future studies, it is suggested that this value is reduced to the extent that the mesh size allows. Once again, it is noted that the mesh size ultimately becomes the limiting factor.

Overall, it is inferred that the 1.5-19.3mm/s range (indicated by red dotted lines in Figure 49) can be used to characterise the average fire spread rate of the whole fire event but show limited applicability in situations where the transient fire spread fluctuations impact on the outcome significantly. The results also reveal certain patterns in the burning behaviour such as the end-of-compartment flashover, the stable fire spread rate close to openings, and radial to linear fire spread flame front. One of the potential avenues of research could thus be to devise a procedure to predict the fire spread rate first, and then plug the results into travelling fire equations.

7 CONCLUSION AND FUTURE WORKS

During the course of this study, several CFD simulations displaying travelling fire behaviour were investigated and compared to the Travelling Fire Methodology. The results confirmed that the position and size of ventilation openings, the HRRPUA, compartment height and geometry had a strong impact on the travelling fire behaviour. Most markedly, the position of the ventilation was found to lead to drastically different fire behaviours; compartments with tunnel-like configuration showed a relatively homogenous burning while compartments with recesses exhibited flashover events prior to burnout.

Flow field results revealed that the flashover occurred because hot smoke was trapped between the walls of the compartment and the advancing flame front. Lesser overall thermal exposure was noted in cases where smoke could readily flow out of the compartment. Due to this phenomenon, certain points within the compartment were found to be subjected to elevated flame temperatures multiple times implying more severe thermal damage on the structure at those locations. The simulations also identified that ceiling jets extended towards the openings, causing those sections of the ceilings to be exposed to a larger thermal load. The scenarios studied also showed that there was no apparent direct correlation between opening dimensions and the peak temperatures recorded. There was a substantial difference in temperature-time profiles resulting from changes in ventilation conditions during the course of a fire event.

Secondly, the ceiling adiabatic surface temperatures from the simulations and the results obtained from the TFM were compared. The predictive capability of the TFM was found to be limited to specific situations because of its inherent assumptions. The fixed fire spread rate assumption was criticized and was shown not to be consistent with travelling fire behaviour by demonstrating the non-uniformity of the fire spread rate in the simulations run. An attempt to improve the TFM was carried out by adapting the Hasemi ceiling jet model to the TFM but produced mitigated results due to the presence of highly non-axisymmetric ceiling jets. Furthermore, it was inferred that far field temperatures were consistently underpredicted by the TFM because it was based on Alpert's correlation which had been developed in an unconfined ceiling setting. It was also noted that the TFM did not account for differences in temperatures that might occur across the cross-section of a compartment, as seen in Case 2.

While the results and findings discussed in this work shed some light on the phenomena observed during travelling fire behaviour, this thesis exposes many more aspects of travelling fires that have yet to be explored and may give way to more research. First and foremost, a series of reduced scaled experiments would allow for validation of the findings obtained and impart more confidence in the inferences made thus far. More importantly, such experiments might reveal phenomena not replicated by the simulations.

A comparative study with other travelling fire methods, such as those enumerated in the literature review section is proposed as a means to gain a more comprehensive overview of the current methods available. These methods could potentially contain clues as to how to improve the TFM currently in use in the thesis. Moreover, a combination of methods could be sought to address the limitations of each method.

With regards to the FDS simulations, the running of the simulations on finer mesh sizes is strongly advised in future studies. The simulations showed thermal runaway due to slight temperature overpredictions in the early stages of the fire. Furthermore, it was concluded that more accurate fire spread rates could be obtained by refining the mesh size and utilising smaller fuel packages. By

devoting more compute power and time for such research, it would be possible to track parameters at a much more granular level.

Moreover, the simulations performed in this thesis were relatively simple in design and do not reflect a furnished open-plan compartment. As highlighted in the thesis, the conditions inside the enclosure were found to be very sensitive to ventilation and geometry. It would thus be interesting to conduct additional simulations that would model the presence of ceiling obstructions, ignition of fuel at the corner of the compartment, presence of non-uniform fuel loads, suppression system interaction and smoke extraction systems.

Additionally, due to the significant external flaming occurring outside of the compartment, it is proposed that the thermal exposure of exterior walls and possibility of vertical fire spread to other floors be explored in further studies. Further research is especially warranted in this case because the results showed that a large amount of unburnt volatiles were produced inside the compartment; large compartments could thus cause more severe external flaming than a typical room. In the same vein, the use of FDS to quantify the heat flux and HRR burning outside the compartment could be useful. Finally, further investigation and quantification of the thermal effects on the structure could be carried out using Finite Element Methods (FEM), as a research tool, or to assist engineers in gauging the extent of damage such fires could have in the built environment at a structural level.

Having inferred from numerical results the strong influence of ventilation conditions on both the extent and speed of fire spread, it is evident that further research and experimental work is needed to reinforce current temperature-time predictive methods. The thesis work showed that events such as window breakages could significantly change the fire development, reiterating the complexity of fires in large enclosures. Although it is acknowledged that the computational requirements are limiting factors in the accuracy of the numerical simulations, the TFM did not conservatively predict the thermal exposure of the ceiling in the simulations run. While the inferences made so far are substantiated through the numerical study, the need for validation experiments coupled with refined simulations are critical to a better understanding of travelling fires.

8 ACKNOWLEDGEMENTS

I would like to express my gratitude to all those who have helped and supported me throughout this process. I am indebted to Prof. Dr Ir Bart Merci, Prof Dr Ir arch Emmanuel Annerel, and Dr Karim Van Maele for their support, enthusiasm and guidance throughout the course of this thesis. Their perceptive comments and ideas were of great assistance to me in accomplishing this work. I extend my thanks to all those involved in the IMFSE course, for having shaped an exciting and enriching two years. Special thanks go to Dr. Stephen Welch for his guidance on travelling fires and Junyi Li for his help on operating the HPC infrastructure.

I am grateful to my family and friends for their support that has motivated me to pursue my studies. Without their help, time and effort, completing this study would not have been possible. Lastly, but most importantly, I thank Fuen, for her constant encouragement during the last two years. You have helped me balance my work and life with your wonderful ideas and delicious treats.

This Master's thesis was carried out on the Vlaams Supercomputer Centrum Ghent University HPC infrastructure.

9 REFERENCES

- [1] J. Stern-Gottfried and G. Rein, "Travelling fires for structural design-Part II: Design methodology," *Fire Saf. J.*, vol. 54, pp. 96–112, Nov. 2012.
- [2] J. Stern-Gottfried and G. Rein, "Travelling fires for structural design-Part I: Literature review," in *Fire Safety Journal*, 2012, vol. 54, pp. 74–85.
- [3] K. Horová, T. Jána, and F. Wald, "Temperature heterogeneity during travelling fire on experimental building," *Adv. Eng. Softw.*, vol. 62–63, pp. 119–130, 2013.
- [4] B. R. Kirby, D. E. Wainman, L. N. Tomlinson, T. R. Kay, and B. N. Peacock, "NATURAL FIRES IN LARGE SCALE COMPARTMENTS," *Int. J. Eng. Performance-Based Fire Codes*, vol. 1, no. 2, pp. 43–58, 1999.
- [5] J. Stern-Gottfried, "Travelling Fires for Structural Design," *Fire Saf. J.*, vol. 54, pp. 74–85, 2011.
- [6] Oakland Fire Department, "Origin and cause report Incident #2016-085231," Oakland, 2017.
- [7] M. D. Engelhardt *et al.*, "Observations from the fire and collapse of the faculty of architecture building, delft university of technology," *Struct. Congr. 2013 Bridg. Your Passion with Your Prof. - Proc. 2013 Struct. Congr.*, no. January 2017, pp. 1138–1149, 2013.
- [8] I. A. Fletcher, S. Welch, D. Alvear, M. Lazaro, and J. A. Capote, "Model-based analysis of a concrete building subjected to fire," in *Advanced Research Workshop on Fire Computer Modelling*, 2007, no. October.
- [9] T. P. McAllister, "Structural Fire Response and Probable Collapse Sequence of the World Trade Centre Building 7," Washington, 2008.
- [10] *Eurocode 1: Actions on Structures Part 1-2 General Actions - Actions on structures exposed to fire*, vol. 1–2. 2002.
- [11] J. Torero, A. Majdalani, C. Abecassis-Empis, and A. Cowlard, "Revisiting the Compartment Fire," *Fire Saf. Sci.*, vol. 11, pp. 28–45, 2014.
- [12] A. Jonsdottir and G. Rein, "Out of Range," *Fire Risk Management*, BRE research publications, pp. 14–17, Dec-2009.
- [13] G. C. Clifton, "Fire Models for Large Firecells," *HERA Rep. R4-83*, no. 54, 1996.
- [14] P. J. Moss and G. C. Clifton, "Modelling of the Cardington LBTF Steel Frame Building Fire Tests," in *Second International Workshop - Structures in Fire*, 2002.
- [15] J. Stern-Gottfried and G. Rein, "Travelling fires for structural design-Part I: Literature review," *Fire Saf. J.*, vol. 54, pp. 74–85, 2012.
- [16] J. Stern-Gottfried, A. Law, G. Rein, M. Gillie, and J. L. Torero, "A Performance Based Methodology Using Travelling Fires for Structural Analysis," in *8th International Conference on Performance-Based Codes and Fire Safety Design Methods*, 2010.
- [17] M. J. Hurley *et al.*, *SFPE Handbook of Fire Protection Engineering*. New York, NY: Springer New York, 2016.
- [18] R. L. Alpert, "Calculation of response time of ceiling-mounted fire detectors," *Fire Technol.*, vol. 8, no. 3, pp. 181–195, Aug. 1972.
- [19] S. Welch, A. Jowsey, S. Deeny, R. Morgan, and J. L. Torero, "BRE large compartment fire tests-

- Characterising post-flashover fires for model validation," *Fire Saf. J.*, vol. 42, no. 8, pp. 548–567, Nov. 2007.
- [20] N. ; Johansson, J. ; Wahlqvist, and P. Van Hees, "Simple Ceiling Jet Correlation Derived from Numerical Experiments," in *13th International Interflam Conference*, 2013, pp. 61–72.
- [21] X. Dai, S. Welch, and A. Usmani, "Structural implications due to an extended travelling fire methodology (ETFM) framework using SIFBuilder," *10th Int. Conf. Struct. Fire SIF'18*, no. June 6-8, pp. 455–462, 2018.
- [22] E. Rackauskaite, C. Hamel, A. Law, and G. Rein, "Improved Formulation of Travelling Fires and Application to Concrete and Steel Structures," *Structures*, vol. 3, pp. 250–260, Aug. 2015.
- [23] M. J. Peatross and C. L. Beyler, "Ventilation Effects on Compartment Fire Characterization."
- [24] Y. Utiskul, J. G. Quintiere, A. S. Rangwala, B. A. Ringwelski, K. Wakatsuki, and T. Naruse, "Compartment fire phenomena under limited ventilation," *Fire Saf. J.*, vol. 40, no. 4, pp. 367–390, Jun. 2005.
- [25] J. G. Quintiere, "Fire behavior in building compartments," *Proc. Combust. Inst.*, vol. 29, no. 1, pp. 181–193, 2002.
- [26] I. Thomas, K. Moinuddin, and I. Bennetts, "Fire development in a deep enclosure," *Fire Saf. Sci.*, pp. 1277–1288, 2005.
- [27] B. Karlsson and J. G. Quintiere, *Enclosure fire dynamics*, 2nd ed., no. 1. Washington: CRC Press LLC, 2000.
- [28] O. Aljumaiah, G. Andrews, B. Mustafa, H. Al-qattan, V. Shah, and H. Phylaktou, "Air Starved Wood Crib Compartment Fire Heat Release and Toxic Gas Yields," *Fire Saf. Sci.*, vol. 10, no. 1, pp. 1263–1276, 2011.
- [29] K. E. Chotzoglou, E. K. Asimakopoulou, J. Zhang, and M. A. Delichatsios, "An experimental investigation of burning behaviour of liquid pool fire in corridor-like enclosures," *Fire Saf. J.*, vol. 108, p. 102826, Sep. 2019.
- [30] A. Nadjai, F. Ali, J. Fra, and O. Vassart, "Structures in Fire. SiF'2018," in *Conference Proceedings of the 10th International Conference on Structures in Fire 2018*, 2018, p. 1036.
- [31] J. Wahlqvist and P. van Hees, "Influence of the built environment on design fires," *Case Stud. Fire Saf.*, vol. 5, pp. 20–33, May 2016.
- [32] Y. Z. Li and H. Ingason, "Scaling of wood pallet fires Scaling of wood pallet fires," vol. 88, no. February, pp. 96–103, 2014.
- [33] N. Johansson, "Numerical experiments and compartment fires," *Fire Sci. Rev.*, vol. 3, no. 1, p. 2, Dec. 2014.
- [34] J. P. Hidalgo *et al.*, "The Malveira fire test: Full-scale demonstration of fire modes in open-plan compartments," *Fire Saf. J.*, vol. 108, Sep. 2019.
- [35] "FDS-SMV." [Online]. Available: <https://pages.nist.gov/fds-smv/>. [Accessed: 17-Apr-2020].
- [36] V. Babrauskas, "Free burning fires," *Fire Saf. J.*, vol. 11, no. 1–2, pp. 33–51, Jul. 1986.
- [37] V. Novozhilov, B. Moghtaderi, D. F. Fletcher, and J. H. Kent, "Computational fluid dynamics modelling of wood combustion," *Fire Saf. J.*, vol. 27, no. 1, pp. 69–84, Jul. 1996.
- [38] R. Yuen *et al.*, "A Three-dimensional Mathematical Model For The Pyrolysis Of Wet Wood,"

- Fire Saf. Sci.*, vol. 5, no. January, pp. 189–200, 1997.
- [39] I. Vermesi, M. J. DiDomizio, F. Richter, E. J. Weckman, and G. Rein, “Pyrolysis and spontaneous ignition of wood under transient irradiation: Experiments and a-priori predictions,” *Fire Saf. J.*, vol. 91, pp. 218–225, Jul. 2017.
- [40] Y. Li, “Measurement Of The Ignition Temperature Of Wood,” *Fire Saf. Sci.*, vol. 1, no. 4, pp. 380–385, 1992.
- [41] K. B. McGrattan, “Fire dynamics simulator Technical Reference Guide Volume 1: Mathematical Model,” Gaithersburg, MD, 2019.
- [42] S. B. Pope, *Turbulent Flows*. Cambridge: Cambridge University Press.
- [43] K. B. McGrattan and G. P. Forney, “Fire dynamics simulator (version 4) :,” Gaithersburg, MD, 2004.
- [44] V. Babrauskas, “Glass Breakage in Fires,” *Fire Science and Technology Inc.*, 1997. [Online]. Available: https://www.interfire.org/features/glass_breakage.asp. [Accessed: 06-Apr-2020].
- [45] E. Rackauskaite, C. Hamel, A. Law, and G. Rein, “Improved Formulation of Travelling Fires and Application to Concrete and Steel Structures,” *Structures*, vol. 3, pp. 250–260, Aug. 2015.
- [46] E. Rackauskaite, C. Hamel, A. Law, and G. Rein, “Improved Formulation of Travelling Fires and Application to Concrete and Steel Structures,” *Structures*, vol. 3, pp. 250–260, Aug. 2015.
- [47] E. Rackauskaite, C. Hamel, and G. Rein, “Improved travelling fires methodology - iTFM,” in *Applications of Structural Fire Engineering*, 2017.
- [48] G. Rein *et al.*, “Round-robin study of a priori modelling predictions of the Dalmarnock Fire Test One,” *Fire Saf. J.*, vol. 44, no. 4, pp. 590–602, May 2009.
- [49] U. Wickström, “Adiabatic surface temperature and the plate thermometer for calculating heat transfer and controlling fire resistance furnaces,” *Fire Saf. Sci.*, pp. 1227–1238, 2008.
- [50] M. Heidari, P. Kotsovinos, and G. Rein, “Flame extension and the near field under the ceiling for travelling fires inside large compartments,” *Fire Mater.*, no. February, pp. 1–14, 2019.